## Results

In the Part A study, the 5-HTT occupancies were increased by 35.3 to 86.5% as the dose and plasma concentration of duloxetine were increased (Fig. 1a,b). Mean occupancies were 43.6±8.8% at 5 mg, 71.3±5.3% at 20 mg, 80.6±4.8% at 40 mg, and 81.8±4.3% at 60 mg.

The relationship between plasma concentration of duloxetine and 5-HTT occupancy fitted well at $r$=0.91, $ED_{50}$=7.9 mg, $r$=0.93, $ED_{50}$=3.7 ng/ml (Fig. 1a,b).

The mean 5-HTT occupancies of three subjects, after taking 60 mg of duloxetine orally, were 81.8±4.3% at 6 hr, 71.9±5.7% at 25 hr, and 44.9±5.3% at 53 hr. The time-courses of mean 5-HTT occupancy and mean plasma concentration of duloxetine of these three subjects are shown in Fig. 2.

In the Part B study, the mean 5-HTT occupancies of three volunteers, after taking 60 mg of duloxetine orally for 7 consecutive days, were 84.3+2.8% at 6 h, 71.9+2.6% at 49 h, and 47.1+3.7% at 78 h (Fig. 3).

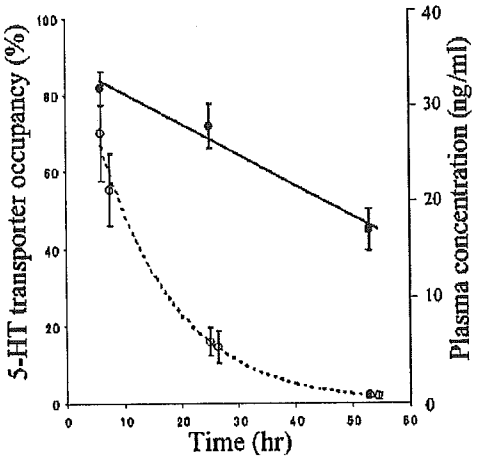


**Fig. 2** Time-course of mean plasma concentration of duloxetine (*open circle*) and mean 5-HTT occupancy (*filled circle*) of three volunteers after taking a single dose of 60 mg of duloxetine. The *dotted line* is a one-exponential function fitting the time-course of plasma concentration, and the *solid line* is a linear function fitting the time-course of 5-HTT occupancy

## Discussion

The present results showed that 5-HTT occupancy was 80.6±4.8% at 40 mg and 81.8±4.3% at 60 mg of single duloxetine administration. By repeated duloxetine administration, 5-HTT occupancy was 84.3±2.8% at 6 h after last administration. Although the threshold of the clinical effects has not been clearly defined for 5-HTT occupancy, over 80% occupancy was reported by the clinical dose of antidepressants during treatment (Meyer et al. 2001, 2004; Suhara et al. 2003). In this study, more than 40 mg of duloxetine was necessary to attain 80% occupancy and a dosage level comparable to the clinical doses of SSRIs for 5-HTT blockage.

The time-course of 5-HTT occupancy and plasma concentration indicated a relatively high (47.1±3.7% at 78 h after repeated 60-mg administration) occupancy remaining even after the plasma concentration had decreased. From linear fitting to the occupancy time-course, about 70% occupancy was estimated at 24 h after a single administration, and about 78% at 24 h after repeated administrations. Sixty milligrams of duloxetine seems to be the optimal dose for keeping a high 5-HTT occupancy level for extended hours.

Several double-blind, placebo-controlled clinical trials of duloxetine have been performed for major depressive disorder, but the dosage differed among the studies. Eighty milligrams/day (40 mg b.i.d.) and 120 mg /day (60 mg b.i.d.) of duloxetine were reported to show efficacy for major depressive disorder (Goldstein et al. 2002; Detke et al. 2004), and a dose of 60 mg a day was also shown to have a clinical effect in the treatment of major depressive disorder (Brannan et al. 2005a,b; Detke et al. 2002a,b).

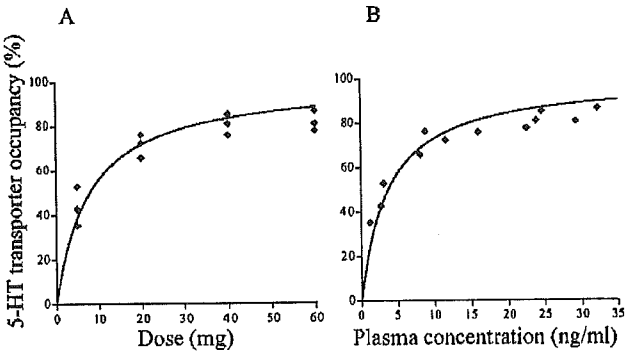


**Fig. 1** Relationship between dose (**a**) and plasma concentration (**b**) just before each PET scan of duloxetine and 5-HTT occupancy. The fitting curves were drawn by the following equation: $\%5\text{-}HTToccupancy = 100 \times C/(ED_{50} + C)$, where %5-HTT occupancy is the percentage of 5-HTT occupied, $ED_{50}$ is a constant, and $C$ is the dose and plasma concentration of duloxetine just before each PET scan

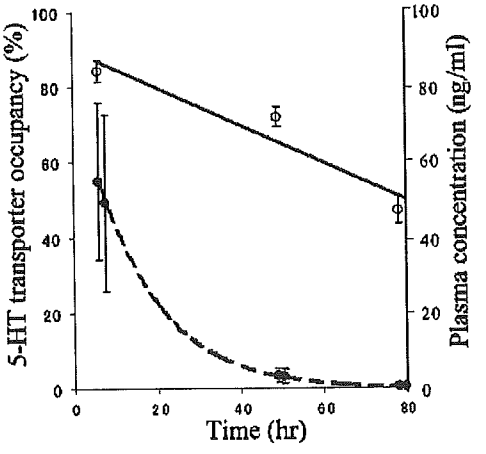


**Fig. 3** Time-course of mean plasma concentration of duloxetine (*open circle*) and mean 5-HTT occupancy (*filled circle*) after taking 60 mg of duloxetine daily for 7 days. The *dotted line* is a one-exponential function fitting the time-course of plasma concentration, and the *solid line* is a linear function fitting the time-course of 5-HTT occupancy

Dosage was determined based on a variety of data concerning the plasma pharmacokinetics and brain penetration (Detke et al. 2002a,b; Wong 1998; Yildiz and Sachs 2001), but sufficient objective evidence regarding dosage and administration schedule appeared to be lacking. Our present results would provide some useful objective evidence to assist in defining clinical dosage settings.

Although duloxetine is both a serotonin and noradrenaline transporter reuptake inhibitor, only 5-HTT occupancy was investigated in this study because an adequate PET ligand for noradrenaline transporter is at present not available.

An in vitro report indicated that duloxetine has greater affinity to 5-HTT (Ki=0.8) than to noradrenaline transporter (Ki=7.5)(Bymaster et al. 2001). As in vivo affinity ($ED_{50}$ values) might be estimated from in vitro binding data (Ki values), noradrenaline transporter occupancy by duloxetine would be about 30% at a dose occupying 80% of 5-HTT. Although the in vitro binding data do not always apply to in vivo binding situations, there is a possibility that higher doses may have some effect through higher blockage of noradrenaline transporter (Chalon et al. 2003, Turcotte et al. 2001). The role of noradrenaline reuptake inhibition for duloxetine needs to be clarified.

In this study, the thalamus was used to measure 5-HTT occupancy because it has the highest specific binding in the brain (Houle et al. 2000). We measured 5-HTT occupancy in the thalamus in our previous study with [$^{11}$C]McN(+)5652 (Suhara et al. 2003), and 5-HTT occupancy has also been reported using [$^{11}$C]DASB in the thalamus and several other regions (Meyer et al. 2004). Regional differences of 5-HTT occupancy should be discussed in the future.

The cerebellum was used as reference tissue for [$^{11}$C] DASB quantification (Ginovart et al. 2001; Ichise et al. 2003). Cerebellar gray matter has recently been suggested to be an optimal reference region because it has very low 5-HTT and its effect on binding potential would not to exceed 7% (Kish et al. 2005; Parsey et al. 2006).

## Conclusions

We investigated 5-HTT occupancy by duloxetine. It was shown that 5-HTT occupancy increased gradually as dose and plasma concentration increased. Forty milligrams and more of duloxetine was necessary to reach 80% occupancy, a level comparable to the clinical doses of SSRIs regarding 5-HTT blockage. 5-HTT occupancy by 60 mg of duloxetine remained high even after the plasma concentration decreased, and it was observed that this dosage given daily can maintain a high level of 5-HTT occupancy.

**Acknowledgement** This research was conducted as LY248686 (duloxetine) phase I study in Japan, and was partially supported by Shionogi and Co., Ltd.

## References

Andree B, Hedman A, Thorberg SO, Nilsson D, Halldin C, Farde L (2003) Positron emission tomographic analysis of dose-dependent NAD-299 binding to 5-hydroxytryptamine-1A receptors in the human brain. Psychopharmacology (Berl) 167:37–45

Brannan SK, Mallinckrodt CH, Detke MJ, Watkin JG, Tollefson GD (2005a) Onset of action for duloxetine 60 mg once daily: double-blind, placebo-controlled studies. J Psychiatr Res 39:161–172

Brannan SK, Mallinckrodt CH, Brown EB, Wohlreich MM, Watkin JG, Schatzberg AF (2005b) Duloxetine 60 mg once-daily in the treatment of painful physical symptoms in patients with major depressive disorder. J Psychiatr Res 39:43–53

Bymaster FP, Dreshfield-Ahmad LJ, Threlkeld PG, Shaw JL, Thompson L, Nelson DL, Hemrick-Luecke SK, Wong DT (2001) Comparative affinity of duloxetine and venlafaxine for serotonin and norepinephrine transporters in vitro and in vivo, human serotonin receptor subtypes, and other neuronal receptors. Neuropsychopharmacology 25:871–880

Chalon SA, Granier LA, Vandenhende FR, Biek PR, Bymaster FP, Joliat MJ, Hirth C, Potter WZ (2003) Duloxetine increases serotonin and norepinephrine availability in healthy subjects: a double-blind, controlled study. Neuropsychopharmacology 28:1685–1693

Detke MJ, Lu Y, Goldstein DJ, McNamara RK, Demitrack MA (2002a) Duloxetine 60 mg once daily dosing versus placebo in the acute treatment of major depression. J Psychiatr Res 36:383–390

Detke MJ, Lu Y, Goldstein DJ, Hayes JR, Demitrack MA (2002b) Duloxetine, 60 mg once daily, for major depressive disorder: a randomized double-blind placebo-controlled trial. J Clin Psychiatry 63:308–315

Detke MJ, Wiltse CG, Mallinckrodt CH, McNamara RK, Demitrack MA, Bitter I (2004) Duloxetine in the acute and long-term treatment of major depressive disorder: a placebo- and paroxetine-controlled trial. Eur Neuropsychopharmacol 14: 457–470

Farde L, Wiesel FA, Halldin C, Sedvall G (1988) Central $D_2$-dopamine receptor occupancy in schizophrenic patients treated with antipsychotic drugs. Arch Gen Psychiatry 45:71–76

Ginovart N, Wilson AA, Meyer JH, Hussey D, Houle S (2001) Positron emission tomography quantification of [$^{11}$C]-DASB binding to the human serotonin transporter: modeling strategies. J Cereb Blood Flow Metab 21:1342–1353

Goldstein DJ, Mallinckrodt C, Lu Y, Demitrack MA (2002) Duloxetine in the treatment of major depressive disorder: a double-blind clinical trial. J Clin Psychiatry 63:225–231

Houle S, Ginovart N, Hussey D, Meyer JH, Wilson AA (2000) Imaging the serotonin transporter with positron emission tomography: initial human studies with [$^{11}$C]DAPP and [$^{11}$C] DASB. Eur J Nucl Med 27:1719–1722

Ichise M, Liow JS, Lu JQ, Takano A, Model K, Toyama H, Suhara T, Suzuki K, Innis RB, Carson RE (2003) Linearized reference tissue parametric imaging methods: application to [$^{11}$C]DASB positron emission tomography studies of the serotonin transporter in human brain. J Cereb Blood Flow Metab 23:1096–1112

Kish SJ, Furukawa Y, Chang LJ, Tong J, Ginovart N, Wilson A, Houle S, Meyer JH (2005) Regional distribution of serotonin transporter protein in postmortem human brain: is the cerebellum a SERT-free brain region? Nucl Med Biol 32:123–128

Mamo D, Sedman E, Tillner J, Sellers EM, Romach MK, Kapur S (2004) EMD 281014, a specific and potent 5HT2 antagonist in humans: a dose-finding PET study. Psychopharmacology (Berl) 175:382–388

Meyer JH, Wilson AA, Ginovart N, Goulding V, Hussey D, Hood K, Houle S (2001) Occupancy of serotonin transporters by paroxetine and citalopram during treatment of depression: a [$^{11}$C]DASB PET imaging study. Am J Psychiatry 158:1843–1849

Meyer JH, Wilson AA, Sagrati S, Hussey D, Carella A, Potter WZ, Ginovart N, Spencer EP, Cheok A, Houle S (2004) Serotonin transporter occupancy of five selective serotonin reuptake inhibitors at different doses: an [$^{11}$C]DASB positron emission tomography study. Am J Psychiatry 161:826–835

Parsey RV, Kent JM, Oquendo MA, Richards MC, Pratap M, Cooper TB, Arango V, Mann JJ (2006) Acute occupancy of brain serotonin transporter by sertraline as measured by [$^{11}$C]DASB and positron emission tomography. Biol Psychiatry (in press)

Suhara T, Takano A, Sudo Y, Ichimiya T, Inoue M, Yasuno F, Ikoma Y, Okubo Y (2003) High levels of serotonin transporter occupancy with low-dose clomipramine in comparative occupancy study with fluvoxamine using positron emission tomography. Arch Gen Psychiatry 60:386–391

Takano A, Suhara T (2005) The necessary parameters for estimating the time-course of receptor occupancy. Int J Neuropsychopharmacol 8:143–144

Takano A, Suhara T, Yasuno F, Suzuki K, Takahashi H, Morimoto T, Lee YJ, Kusuhara H, Sugiyama Y, Okubo Y (2006) The antipsychotic sultopride is overdosed—a PET study of drug-induced receptor occupancy in comparison with sulpiride. Int J Neuropsychopharmacol (in press)

Tauscher J, Jones C, Remington G, Zipursky RB, Kapur S (2002) Significant dissociation of brain and plasma kinetics with antipsychotics. Mol Psychiatry 7:317–321

Turcotte JE, Debonnel G, de Montigny C, Hebert C, Blier P (2001) Assessment of the serotonin and norepinephrine reuptake blocking properties of duloxetine in healthy subjects. Neuropsychopharmacology 24:511–521

Wilson AA, Garcia A, Jin L, Houle S (2000a) Radiotracer synthesis from [$^{11}$C]-iodomethane: a remarkably simple captive solvent method. Nucl Med Biol 27:529–532

Wilson AA, Ginovart N, Schmidt M, Meyer JH, Threlkeld PG, Houle S (2000b) Novel radiotracers for imaging the serotonin transporter by positron emission tomography: synthesis, radiosynthesis, and in vitro and ex vivo evaluation of $^{11}$C-labeled 2-(phenylthio)araalkylamines. J Med Chem 43:3103–3110

Wong DT (1998) Duloxetine (LY248686): an inhibitor of serotonin and noradrenaline uptake and an antidepressant drug candidate. Expert Opin Investig Drugs 7:1691–1699

Yasuno F, Hasnine AH, Suhara T, Ichimiya T, Sudo Y, Inoue M, Takano A, Ou T, Ando T, Toyama H (2002) Template-based method for multiple volumes of interest of human brain PET images. Neuroimage 16:577–586

Yildiz A, Sachs GS (2001) Administration of antidepressants. Single versus split dosing: a meta-analysis. J Affect Disord 66:199–206

0022-3565/06/3162-647–653$20.00
THE JOURNAL OF PHARMACOLOGY AND EXPERIMENTAL THERAPEUTICS
Vol. 316, No. 2
88328/3082565
JPET 316:647–653, 2006
*Printed in U.S.A.*


# In Vivo Evaluation of P-glycoprotein Function at the Blood-Brain Barrier in Nonhuman Primates Using [$^{11}$C]Verapamil

Young-Joo Lee,[1] Jun Maeda, Hiroyuki Kusuhara, Takashi Okauchi, Motoki Inaji, Yuji Nagai, Shigeru Obayashi, Ryuji Nakao, Kazutoshi Suzuki, Yuichi Sugiyama, and Tetsuya Suhara

*The Graduate School of Pharmaceutical Sciences, the University of Tokyo, Bunkyo-ku, Tokyo, Japan (Y.-J. L., H.K., Y.S.); Brain Imaging Project, National Institute of Radiological Sciences, Chiba, Japan (J.M., T.O., M.I., Y.N., S.O., T.S.); and Department of Medical Imaging, National Institute of Radiological Sciences, Chiba, Japan (R.N., K.S.)*

Received April 21, 2005; accepted November 16, 2005

**ABSTRACT**

P-glycoprotein (P-gp) is a major efflux transporter contributing to the efflux of a range of xenobiotic compounds at the blood-brain barrier (BBB). In the present study, we evaluated the P-gp function at the BBB using positron emission tomography (PET) in nonhuman primates. Serial brain PET scans were obtained in three rhesus monkeys after intravenous administration of [$^{11}$C]verapamil under control and P-gp inhibition conditions ([PSC833 ([3′-keto-Me-Bmt$^1$]-[Val$^2$]-cyclosporin) 20 mg/kg/2 h]). The parent [$^{11}$C]verapamil and its metabolites in plasma were determined by HPLC with a positron detector. The initial brain uptake clearance calculated from the integration plot was used for the quantitative analysis. After intravenous administration, [$^{11}$C]verapamil was taken up rapidly into the brain (time to reach the peak, 0.58 min). The blood level of [$^{11}$C]verapamil decreased rapidly, and it underwent metabolism with time. The inhibition of P-gp by PSC833 increased the brain uptake of [$^{11}$C]verapamil 4.61-fold (0.141 versus 0.651 ml/g brain/min, $p < 0.05$). These results suggest that PET measurement with [$^{11}$C]verapamil can be used for the evaluation of P-gp function at the BBB in the living brain.

The blood-brain barrier (BBB), formed by brain-capillary endothelial cells, is a functional barrier responsible for restricting the entry of compounds from the circulating blood to the brain parenchyma cells (Reese and Karnovsky, 1967). The highly developed tight junctions between the adjacent brain cerebral endothelial cells are an anatomical feature of the BBB that minimizes the nonspecific penetration of compounds via paracellular route (Pardridge, 1988). In addition to this physical barrier, metabolic enzymes and active efflux transporters on this barrier also play important roles in BBB function. P-glycoprotein (P-gp), a 170-kDa membrane protein that is responsible for the multidrug resistance of tumor cells, is a major efflux transporter contributing to the efflux of a range of xenobiotic compounds in the circulating blood at the BBB (Schinkel et al., 1994; Tamai and Tsuji, 2000; Kusuhara and Sugiyama, 2001; Hirrlinger et al., 2002). Interestingly, P-gp may also be involved in the efflux of β-amyloid and has been suspected to play a role in Alzheimer's disease (Lam et al., 2001; Vogelgesang et al., 2002). In addition, a drug-drug interaction involving P-gp inhibition at the BBB has also been suggested (Sadeque at al., 2000). In a clinical study, when loperamide was administered with quinidine, a known P-gp inhibitor, respiratory depression by loperamide was induced (Sadeque at al., 2000). It is speculated that this is caused by modulation of the P-gp-mediated efflux by quinidine. Furthermore, a genetic polymorphism (C3435T) of P-gp has been reported to be associated with drug resistance in patients with epilepsy (Siddiqui et al., 2003), although a controversial result was reported recently (Tan et al., 2004). Such a genetic polymorphism may be associated with interindividual differences in drug concentration in the central nervous system.

This study was performed through the Advanced and Innovational Research program in Life Sciences from the Ministry of Education, Culture, Sports, Science and Technology, Japan. This work was also partially supported by a research grant from the Society of Japanese Pharmacopoeia and the Minister of Health, Labor and Welfare.

[1] Current affiliation: College of Pharmacy, Kyung Hee University, Seoul, Korea.

Article, publication date, and citation information can be found at http://jpet.aspetjournals.org.
doi:10.1124/jpet.105.088328.

**ABBREVIATIONS:** BBB, blood-brain barrier; ANOVA, analysis of variance; AUC, area under the curve; $C_{max}$, maximal concentration; HPLC, high-pressure liquid chromatography; MRI, magnetic resonance image; PET, positron emission tomography; P-gp, P-glycoprotein; PSC833, [3′-keto-Me-Bmt$^1$]-[Val$^2$]-cyclosporin; $T_{max}$, time to reach the $C_{max}$.

These clinical reports prompted a growing interest in the quantitative evaluation of P-gp function in living human brain.

Recently, in vivo evaluation of P-gp function was proposed using an imaging method with [$^{11}$C]colchicine, [$^{11}$C]carvedilol, [$^{18}$F]paclitaxel, and [$^{11}$C]verapamil (Elsinga et al., 2004). Hendrikse et al. (1998) demonstrated in rodents that the brain uptake of the P-gp substrate [$^{11}$C]verapamil was increased after pretreatment with cyclosporin A, a P-gp inhibitor, and they showed that that the distribution volume, estimated by Logan plot, was increased by pretreatment with cyclosporin A (Bart et al., 2003; Elsinga et al., 2004). As for human studies, Sasongko et al. (2005) demonstrated that the ratio of the area under the curve (AUC) of the brain concentration to that of blood concentration was increased in the presence of cyclosporin A, and Kortekaas et al. (2005) reported that the distribution volume of [$^{11}$C]verapamil in the midbrain was increased in Parkinson's disease patients compared with controls. In the present study, the P-gp function at the BBB was evaluated in rhesus monkeys by PET using [$^{11}$C]verapamil, with or without a potent P-gp inhibitor PSC833. PSC833 treatment caused a significant increase in the brain uptake clearance of [$^{11}$C]verapamil, which was determined using integration plot analysis using initial brain and blood concentration data.

## Materials and Methods

**Chemicals.** The P-gp inhibitor PSC833 (Valspodar) was kindly supplied by Novartis (Basel, Switzerland) and was dissolved in Intralipid (Lo et al., 2001) (oil in water emulsion droplet; Otsuka Pharmaceutical, Tokyo, Japan). [$^{11}$C]Verapamil was synthesized from norverapamil (Eisai Co. Ltd., Tokyo, Japan) as described previously (Wegman et al., 2002) and diluted with approximately 2 to 3 ml 0.9% saline containing 0.75% polyoxyethylenemonosorbitan oleate and 1% ascorbic acid. The specific radioactivity of [$^{11}$C]verapamil used in all experiments ranged from 28.3 to 79.7 GBq/$\mu$mol (47.6 ± 17.3 GBq/$\mu$mol, mean ± S.D., radiochemical purity is over 95%).

**Animals.** Three young male rhesus monkeys (Macaca mulatta) weighing approximately 6.0 to 6.7 kg were used. The monkeys were maintained and handled in accordance with recommendations by the United States National Institutes of Health and our own guidelines (National Institute of Radiological Sciences, Chiba, Japan). The study was approved by the Animal Ethics Committee of the National Institute of Radiological Sciences. A magnetic resonance image (MRI) of each monkey brain was obtained beforehand.

**PET Scan.** All PET scans were performed using a high-resolution SHR-7700 PET camera (Hamamatsu Photonics, Shizuoka, Japan) designed for laboratory animals, which provides 31 transaxial slices 3.6 mm (center-to-center) apart, a 33.1-cm field of view, and spatial resolution of 2.6 mm full width at half-maximum (Watanabe et al., 1997). Monkeys were trained beforehand as being immobilized with the head fixation device to ensure accuracy of repositioning throughout the session (Obayashi et al., 2001). The infusion of PSC833 (20 mg/kg/2 h), a P-gp modulator, or vehicle alone to each monkey was started 1 h before the intravenous administration of [$^{11}$C]verapamil and maintained during the experiment. After administration of [$^{11}$C]verapamil, 0.9% saline was flushed into the catheter line to prevent adsorption or retention of verapamil. Arterial blood sampling (~0.5–1.5 ml) was performed via an indwelling arterial port from the saphenous artery at 10 s, 20 s, 30 s, 45 s, 1 min, 1.5 min, 3 min, 4.5 min, 6 min, 8 min, 10 min, 15 min, 20 min, 30 min, 45 min, and 60 min after administration, and the radioactivity in the blood was counted in a well-type $\gamma$-scintillation counter. Radioactivity was corrected for decay. After transmission scans for attenuation correction for 30 min, a dynamic emission scan in enhanced 2D mode was performed for 60 min (10 × 12 s, 30 × 6 s, 1 × 5 min, 2 × 5 min, and 5 × 8 min; a total of 36 frames). [$^{11}$C]Verapamil was administered via the saphenous vein as a single bolus at the start of the emission scan. The injected doses of [$^{11}$C]verapamil were 65.8 ± 11.5 MBq/kg (mean ± S.D.). The PET scans were separated by at least 4-week intervals and randomized for each monkey.

**Metabolite Analysis.** Arterial blood samples were collected at 1, 3, 6, 10, 15, 30, and 60 min after administration of [$^{11}$C]verapamil. Plasma was obtained by centrifugation and deproteinized with 2 volumes of acetonitrile. The supernatant was analyzed for radioactive components using a high-pressure liquid chromatography (HPLC) system (PU-610A series; GL Sciences, Torrance, CA) with a coupled NaI(Tl) positron detector (Takei et al., 2001) to measure [$^{11}$C]verapamil metabolites. Isocratic elution was performed with a reversed-phase semipreparative $\mu$-Bondpak C18 column (7.8 × 300 mm i.d.; Waters, Milford, MA). The mobile phase consisted of a mixture of acetonitrile and 0.1 M ammonium acetate (70:30 v/v). The flow rate was 5 ml/min, and the injected sample size was 1.0 ml. The elute was monitored by ultraviolet absorbance at 254 nm and coupled NaI(Tl) positron detection. The percentage of parent radioactivity was determined from the activity of the parent verapamil with respect to the $^{11}$C radioactivity in the chromatogram.

**PET Data Analysis.** All emission scan images were reconstructed with a 4.0-mm Hann filter, and regions of interest were placed on the whole cerebrum using PET Analyzer (in-house software, National Institute of Radiological Sciences; Maeda et al., 2001), and MRI information on each monkey. The summation images of [$^{11}$C]verapamil from 0 to 5 min were coregistered on the magnetic resonance images by means of statistical parametric mapping (SPM 2; Welcome Department of Cognitive Neurology, London, UK), and then the volume images were processed with Virtual Place TM (AZE Ltd. Tokyo, Japan). The decay-corrected $^{11}$C radioactivity was normalized to the injected dose (% dose). The maximal $^{11}$C radioactivity in the cerebrum ($C_{max\_cereb}$) and the time to reach the $C_{max\_cereb}$ ($T_{max\_cereb}$) were obtained from the time-$^{11}$C radioactivity data. The AUC was calculated for brain and blood, and it was calculated using data from 0 to 4.5 min after administration to minimize the bias by metabolites.

**Integration Plot.** The initial brain uptake was measured over a short period (~1–4.5 min) using integration plot method. The uptake rate of [$^{11}$C]verapamil can be described by the following equation,

$$\frac{X_{t,cereb}}{C_{t,blood}} = CL_{uptake} \times \frac{AUC_{(0\sim t)}}{C_{t,blood}} + V_E \quad (1)$$

where $CL_{uptake}$ is the brain uptake clearance based on the blood $^{11}$C radioactivity, $X_{t,cereb}$ is the amount of $^{11}$C radioactivity in the cerebrum at time $t$, and $C_{t,blood}$ is the blood concentration calculated from $^{11}$C radioactivity. $AUC_{(0-t)}$ represents the area under the blood concentration curve from 0 to $t$, and $V_E$ represents the initial distribution volume in the brain at time 0. $V_E$ was obtained from the $y$-intercept of the integration plot and includes the distribution volume in blood residing within the brain as well as the initial distribution volume of [$^{11}$C]verapamil in the brain rapidly equilibrating with that in blood. Therefore, the $CL_{uptake}$ value can be obtained from the initial slope of a plot of $X_{t,cereb}/C_{t,blood}$ versus $AUC_{(0\sim t)}/C_{t,blood}$, designated as the integration plot (Kim et al., 1988).

**Inhibition of P-gp Function.** The effect of PSC833, a P-gp modulator, was evaluated based on the normalized time-activity curves of brain and blood for the three monkeys, with and without PSC833 administration. PSC833 was infused at a dose of 20 mg/kg/2 h starting 1 h before intravenous administration of [$^{11}$C]verapamil and maintained until the end of the experiment (Song et al., 1999; Rodriguez et al., 2004). In a control experiment, drug vehicle was infused in the same manner. Differences were considered statistically significant when $p < 0.05$ using a one-sided paired $t$ test, with the exception of the time course results in which two-way analysis of variance was used.

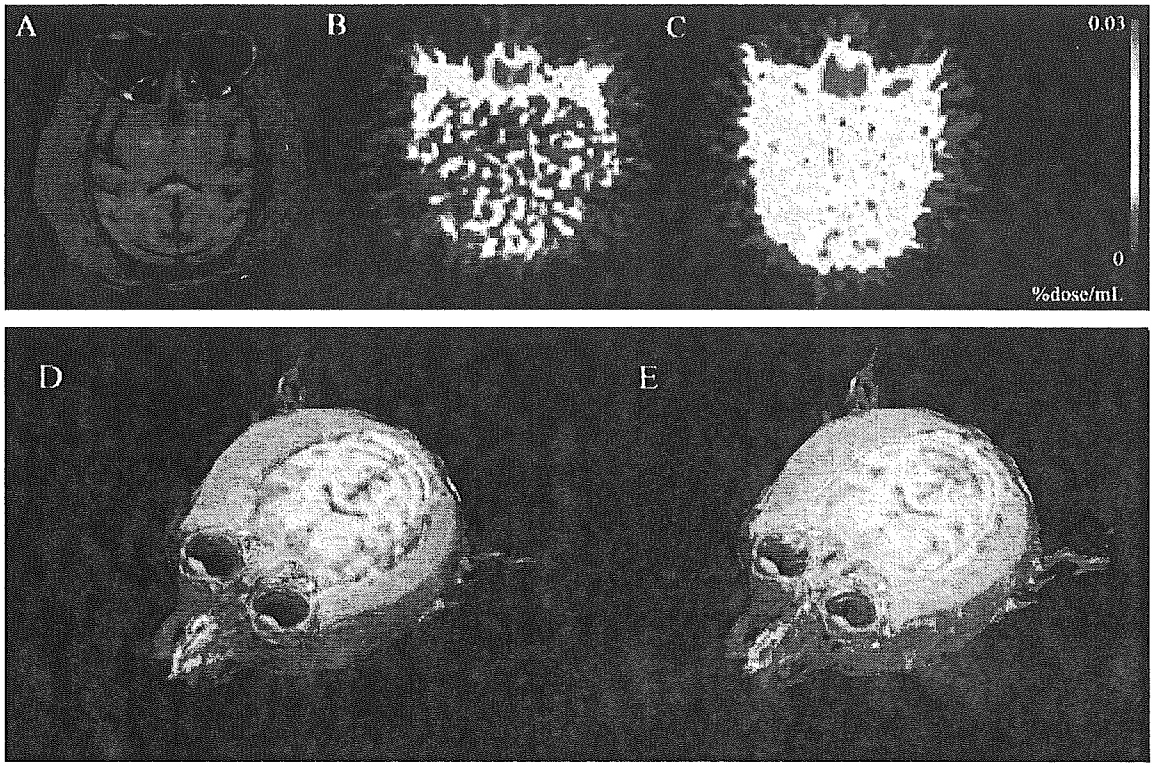


**Fig. 1.** A typical MRI and a color-coded PET image after administration of [$^{11}$C]verapamil. Horizontal slices of the brain MRI scans (A) and corresponding summation of PET images (B and C, up to 5 min) of the cerebral $^{11}$C radioactivity uptake in one animal. The reconstructed MRI-PET image is also shown to assist intuitive understanding (D and E). B and D represent the control state, and C and E are the P-gp inhibition conditions obtained after PSC833 administration.

## Results

**The Distribution of [$^{11}$C]Verapamil in the Brain.** A control PET image (Fig. 1B) accompanied by a corresponding morphological MRI (Fig. 1A) showed the uptake of $^{11}$C radioactivity in the monkey brain. Higher uptake of $^{11}$C radioactivity was observed in the brain after PSC833 treatment (Fig. 1C, PSC833-treated). Brain uptake was also clearly identified from PET/MRI-coregistered images (Fig. 1, D and E). The time-activity curves in the cerebrum are shown in Fig. 2. The $^{11}$C radioactivity in the cerebrum peaked at 0.58 min after intravenous administration of [$^{11}$C]verapamil and remained almost constant at this level up to 60 min. Only limited amount of $^{11}$C radioactivity (0.0105 ± 0.0006% dose/g brain, $C_{max\_cereb}$, mean ± S.D.) was transported into the cerebrum.

Treatment with PSC833 significantly increased the $^{11}$C radioactivity uptake in the cerebrum (two-way ANOVA, $p < 0.05$). The cerebrum AUC ($AUC_{cereb}$) of the PSC833 treatment group was significantly greater than that of the control group (1.96-fold) (Table 1; $p < 0.05$). The $C_{max\_cereb}$ of the PSC833 treatment group was also significantly higher than that of the control group (1.57-fold) (Table 1, $p < 0.05$). The $T_{max\_cereb}$ was not changed by treatment with PSC833 (Table 1).

**Blood Profile and Metabolism of [$^{11}$C]Verapamil.** The time-$^{11}$C radioactivity in the blood is shown in Fig. 3. The $^{11}$C radioactivity in the blood fell quickly up to 3 min and then remained constant or slightly increased. Treatment with PSC833 did not affect the blood $^{11}$C radioactivity profile (two-way ANOVA). The blood AUC ($AUC_{blood}$) of the PSC833 treatment group was similar to that of the control group (Table 1).

A chromatogram of the HPLC analysis of [$^{11}$C]verapamil, with or without treatment with PSC833, is shown in Fig. 4A. The retention time of verapamil was approximately 7 to 8 min. The fraction of intact verapamil decreased with time (Fig. 4B). At 10 min after administration, on average, approximately 25% of the radioactivity in plasma was the metabolite of [$^{11}$C]verapamil in the control group and intact verapamil represented approximately 50% of the radioactivity in the plasma of the control group 30 min after administration

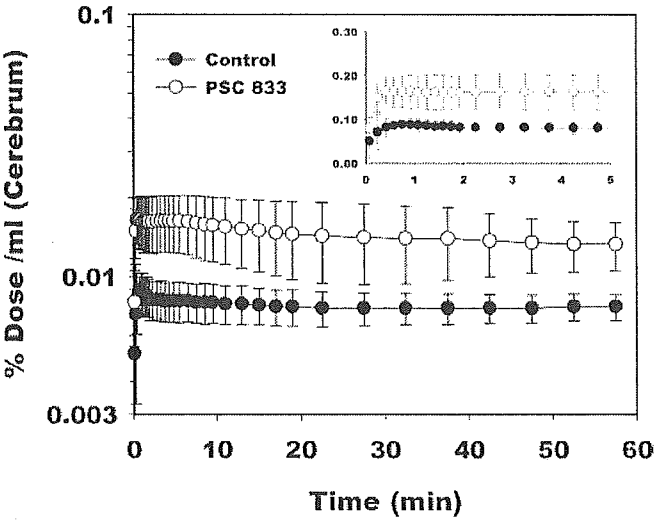


**Fig. 2.** The $^{11}$C radioactivity time curves in cerebrum. The inset shows the detail curves in the early time period (mean ± S.D., $n = 3$). The treatment with PSC833 clearly increases the $^{11}$C radioactivity in the cerebrum (two-way ANOVA, $p < 0.05$).

TABLE 1

Pharmacokinetic parameters of [$^{11}$C]verapamil after intravenous administration, with or without PSC833 (20 mg/kg/2 h)

The $AUC_{blood}$ and $AUC_{cereb}$ were calculated from 0 to 4.5 min after the administration using data shown in Figs. 2 and 3. $CL_{uptake}$ and $V_E$ were obtained from Figure 5. The values represent mean ± S.D. ($n$ = 3). Data in parentheses indicate values from individual animals.

| Pharmacokinetic Parameter | Control | + PSC833 Treatment |
|---|---|---|
| $AUC_{blood}$ (% dose × min/ml) | 0.0567 ± 0.0145 (0.0461, 0.0733, 0.0507) | 0.0535 ± 0.0331 (0.0418, 0.0279, 0.0909) |
| $AUC_{cereb}$ (% dose × min/g) | 0.0365 ± 0.0039 (0.0407, 0.0359, 0.0328) | 0.0713 ± 0.0169* (0.0795, 0.0519, 0.0827) |
| $C_{max\_cereb}$ (% dose/g) | 0.0105 ± 0.0006 (0.0104, 0.00989, 0.0112) | 0.0166 ± 0.0033* (0.0185, 0.0128, 0.0192) |
| $T_{max\_cereb}$ (min) | 0.58 ± 0.44 (1.08, 0.42, 0.25) | 0.59 ± 0.29 (0.92, 0.42, 0.42) |
| $CL_{uptake}$ (ml/g/min) | 0.141 ± 0.043 (0.185, 0.139, 0.100) | 0.651 ± 0.333* (0.937, 0.731, 0.285) |
| $V_E$ (ml/g) | 0.243 ± 0.130 (0.286, 0.0971, 0.346) | 0.436 ± 0.279 (0.402, 0.731, 0.176) |

* A statistically significant difference was observed ($t$ test, $P < 0.05$).

(Fig. 4B). Treatment with PSC833 slightly increased the metabolite fraction in plasma (Fig. 4B; two-way ANOVA, $p < 0.05$). The inset in Fig. 3 shows the time-activity curves of intact [$^{11}$C]verapamil in plasma. The plasma radioactivity profile of intact [$^{11}$C]verapamil was not affected by treatment with PSC833 (two-way ANOVA).

**The Brain Uptake Clearance of [$^{11}$C]Verapamil and Effect of PSC833.** Integration plots of the control and PSC833 treatment studies of the three monkeys are shown in Fig. 5, A through C. The integration plots were linear over a short period, which varied from 1 min to 4.5 min, depending on the subject and with or without PSC833 treatment. During this period, the metabolite of [$^{11}$C]verapamil accounted for less than 12.5% $^{11}$C radioactivity. The initial brain uptake of the control group was 0.141 ml/g/min (0.141 ± 0.043, mean ± S.D.), and this was increased after PSC833 treatment (0.651 ± 0.333 ml/g brain/min, mean ± S.D., $p < 0.05$). The $V_E$ was not changed by PSC833 treatment (Table 1). The $AUC_{cereb}/AUC_{blood}$ ratio of $^{11}$C radioactivity was increased 2.31-fold in the presence of PSC833.

## Discussion

In this study, we evaluated the P-gp function at the BBB in vivo using PET with [$^{11}$C]verapamil. Recently, the use of imaging techniques, such as single photon emission-computed tomography and PET using [$^{11}$C]colchicine, [$^{11}$C]carvedilol, [$^{18}$F]paclitaxel, and [$^{64}$Cu]complexes and [$^{68}$Ga]complexes and [$^{99m}$Tc]complexes, has been suggested for the noninvasive evaluation of P-gp function in vivo (Elsinga et al., 2004). Among these compounds, [$^{11}$C]verapamil is a well characterized PET ligand for evaluating P-gp function at the BBB (Hendrikse et al., 1998, 1999), and verapamil can be easily labeled with $^{11}$C using commercially available norverapamil (Wegman et al., 2002).

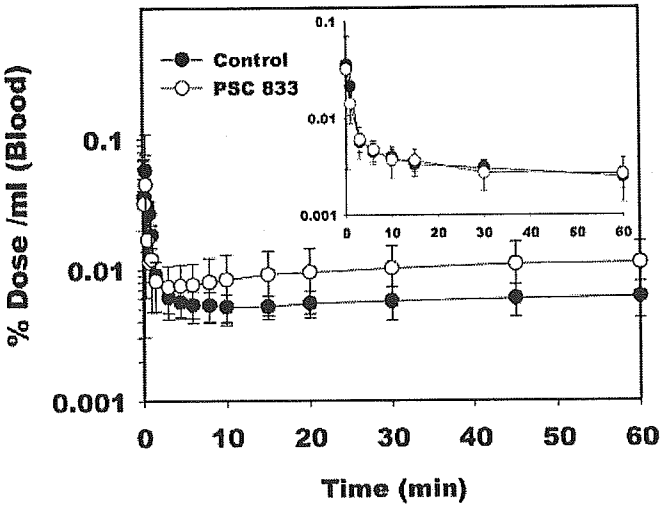


**Fig. 3.** The [$^{11}$C]radioactivity and intact (inset) [$^{11}$C]verapamil activity-time curves in cerebrum and blood. The time-$^{11}$C radioactivity and intact [$^{11}$C]verapamil activity curves in blood are similar for both the control and PSC833 treatment groups (mean ± S.D., $n$ = 3).

After intravenous administration of [$^{11}$C]verapamil, it was rapidly distributed in the brain over a short period and then was eliminated slowly (Fig. 2). Apparently, the $^{11}$C radioactivity reached a distributional pseudoequilibrium within a short period (Fig. 3). This is similar to earlier results obtained in rats (Hendrikse et al., 1999). The uptake of $^{11}$C radioactivity into the cerebrum increased after PSC833 treatment (Figs. 1 and 2). PSC833 treatment increased the $AUC_{cereb}$ and $C_{max\_cereb}$ of $^{11}$C radioactivity compared with the values obtained in the control group (Table 1). These data indicate that the efflux transport by P-gp affects the initial brain uptake and that the inhibition of P-gp-mediated transport increases the brain uptake of P-gp substrates (Kusuhara et al., 1997; Dagenais et al., 2000) and supports recent human brain PET study using [$^{11}$C]verapamil, which was published during the revision process of this manuscript (Sasongko et al., 2005).

The blood concentration-time profile of the $^{11}$C radioactivity was biphasic, exhibiting a rapid reduction within minutes followed by an increase in the $^{11}$C radioactivity (Fig. 3). The increase at later time points was more marked in the PSC833-treated group than in the control group. The $^{11}$C radioactivity in the blood specimens includes unchanged [$^{11}$C]verapamil and its metabolites (Fig. 4A). Approximately 75% of the $^{11}$C radioactivity was unchanged [$^{11}$C]verapamil during the initial 10 min, and the fraction of the unchanged form in the blood specimens rapidly decreased (Fig. 4B). This observation is consistent with the previous reports of verapamil metabolism in humans (Kroemer et al., 1993; von Richter et al., 2000; von Richter et al., 2001) and monkeys (Link, 2003), whereas low levels of the metabolite of [$^{11}$C]verapamil during PET studies have been reported in rodents (Hendrikse et al., 1998, 1999). Because the increase at later time points was not observed in the blood concentration-time profile of unchanged [$^{11}$C]verapamil (Fig. 3, inset), it is likely that the increase is due to the accumulation of metabo-

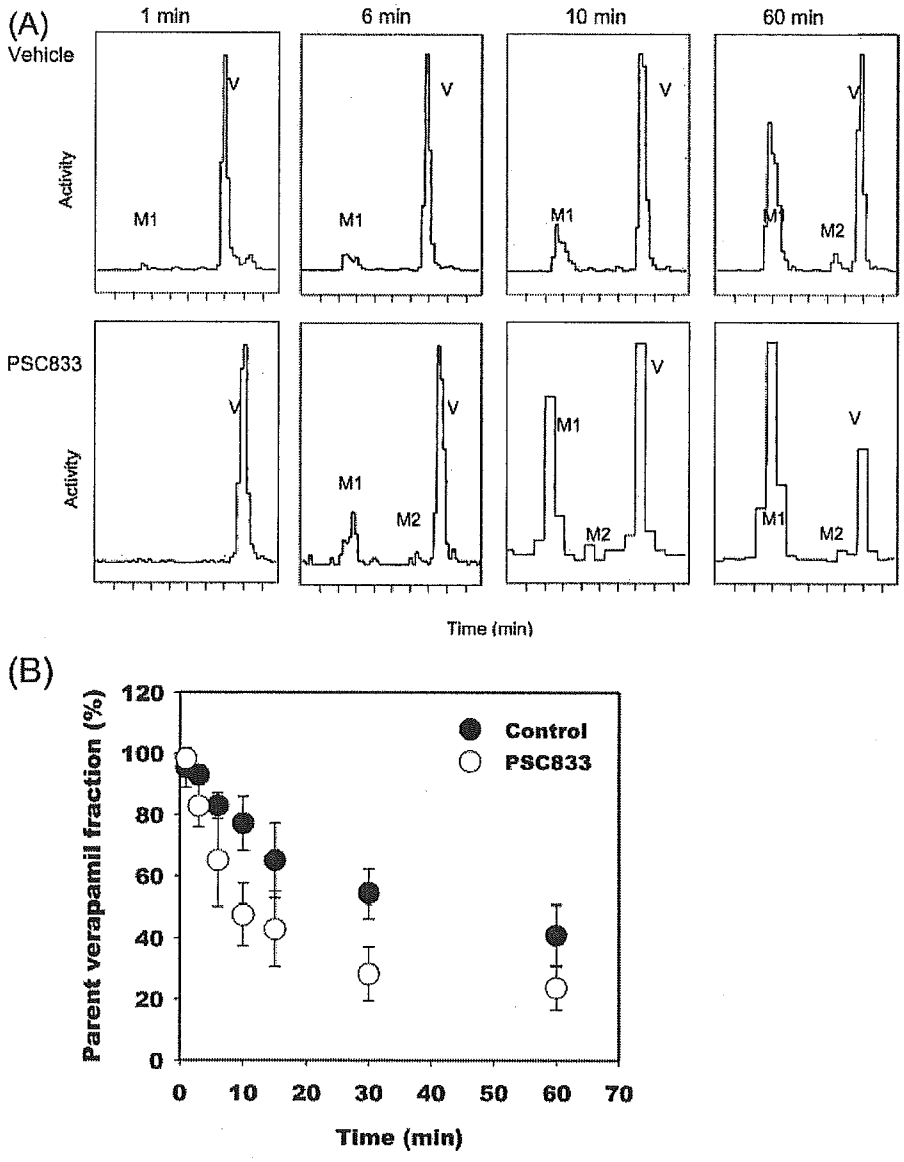


**Fig. 4.** A, typical chromatograms of plasma samples at 1, 6, 10, and 60 min after intravenous administration of [$^{11}$C]verapamil, with or without PSC833. B, parent [$^{11}$C]verapamil fraction of the $^{11}$C radioactivity in plasma. The parent verapamil was detected at approximately 7 to 8 min (V). HPLC analysis suggested that there are at least two metabolites (M1, M2) of verapamil after intravenous administration. The parent fraction of verapamil in plasma fell rapidly with time. At 10 min after administration, on average, approximately 75% of the radioactivity in plasma was due to the parent verapamil in the control group and the parent verapamil represented approximately 50% of the radioactivity in the plasma of the control group 30 min after administration (mean ± S.D., $n$ = 3).

lites in the blood from the peripheral tissues. Since PSC833 is known to be a fairly specific P-gp inhibitor with a low degree of metabolic inhibition (Kawahara et al., 2000) and metabolites of verapamil are also substrates of P-gp with a range of specificities (Pauli-Magnus et al., 2000), PSC833 treatment may cause a delay in the elimination of metabolized verapamil, resulting in marked plasma accumulation of metabolites.

Because we could not separate metabolites from parent verapamil in brain, there is a possibility that different parent/metabolite ratio might exist in the brain compared with blood. To deal with this extensive metabolism of [$^{11}$C]verapamil, we used the initial PET data (~0–4.5min) to avoid any bias from metabolites. Integration plot analysis has been used to obtain a tissue-specific uptake clearance. The initial PET scan data (from 0 to ~1–4.5 min, depending on the subjects) was enough to calculate the initial uptake clearance, during which no extensive metabolism of verapamil was observed (Fig. 4). Figure 5 shows the integration plot of the blood versus tissue time-activity curves in three monkeys (Fig. 5). The $CL_{uptake}$ calculated from the slope of the integration plot increased after treatment with PSC833. This indicates the modulation of P-gp function at the BBB by PSC833 (Table 1) (Kusuhara et al., 1997; Song et al., 1999). The initial brain uptake clearance of [$^{11}$C]verapamil is a sensitive parameter for P-gp function at the BBB. However, the magnitude of the increase observed in PSC833-treated monkeys was not as high as that observed in P-gp knockout mice. This may be explained by incomplete inhibition of P-gp activity by PSC833, variable brain concentration of PSC833 in monkey, and, partly, a species difference in P-gp expression and/or intrinsic efflux transport activity. In fact, PSC833 treatment does not fully inhibit P-gp function at the BBB in mice (Kusuhara et al., 1997). Interestingly, recent human [$^{11}$C]verapamil PET study in the presence of cyclosporin A showed a similar degree of increase in the brain distribution of verapamil by P-gp inhibition. In this study, the $AUC_{cereb}$/$AUC_{blood}$ ratio of $^{11}$C radioactivity was increased 1.88-fold in the presence of cyclosporin A, which was consistent with the present study (2.31-fold) (Sasongko et al., 2005). This supports the belief that the species difference in the role of P-gp

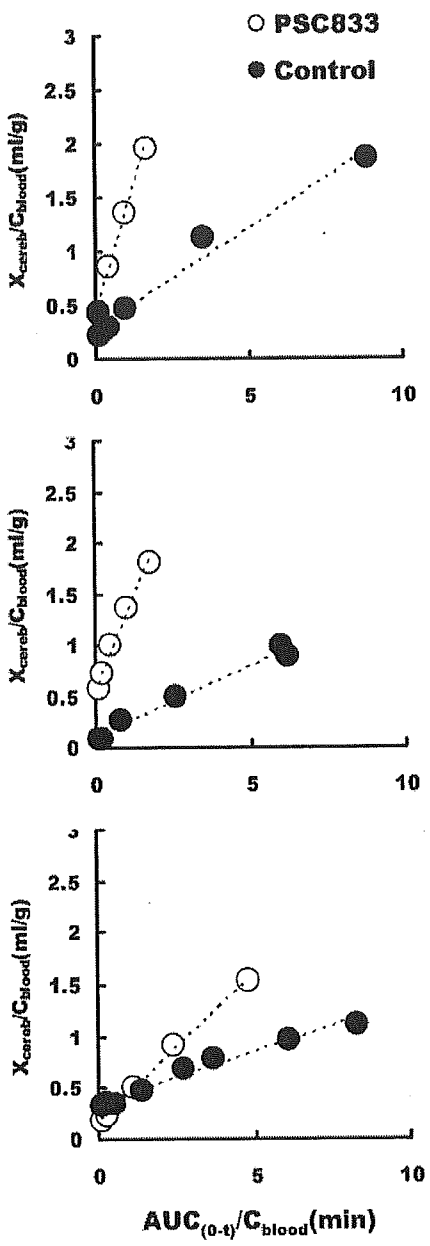


**Fig. 5.** Integration plot of the brain uptake of [$^{11}$C]verapamil for the three monkeys (A, B, and C). The initial brain uptake of the control group was increased after treatment with PSC833 ($t$ test, $p < 0.05$, $n = 3$). The $V_E$ was not changed by PSC833 treatment.

at the BBB may not be very significant between humans and monkeys and suggests the feasibility of a PET study using monkeys to provide information on the human BBB. Unlike the slope, the $y$-intercept of the plot was insensitive to the PSC833 treatment (Table 1). The $y$-intercept represents the initial distribution volume, including the vascular space and rapid adsorption/binding to the vascular surface, which can achieve rapid equilibrium with the blood compartment. Because the initial distribution volume is greater than the vascular space in the brain, estimated to be 35$\mu$l/g brain in 15 adult rhesus monkeys (Eichling et al., 1975), it seems that the adsorption/binding of [$^{11}$C]verapamil to the vascular surface occurs within a short period. The use of integration plot analysis helps in the quantitative investigation of P-gp function at the BBB without any interference from the rapid and extensive metabolism of [$^{11}$C]verapamil, which makes it inappropriate to use common graphical methods that need data obtained from long-term sampling (Logan, 2003).

In conclusion, we have been able to evaluate P-gp function at the BBB in nonhuman primates, using [$^{11}$C]verapamil as a PET ligand and integration plot method. P-gp at the BBB has attracted much interest from a clinical point of view; i.e., drug-drug interactions and the effects of genetic polymorphisms. Therefore, in future, PET studies using [$^{11}$C]verapamil will be a powerful tool for evaluating P-gp function at the BBB in a noninvasive manner.

**Acknowledgments**

We thank the members of the Cyclotron Unit and Radiopharmaceutical and Radiopharmacological Section for operation of the cyclotron and the production of radioisotopes, Novartis Pharm AG for its kind gift of PSC833, and Eisai Co. Ltd. for its kind gift of norverapamil.

**References**

Bart J, Willemsen AT, Groen HJ, van der Graaf WT, Wegman TD, Vaalburg W, de Vries EG, and Hendrikse NH (2003) Quantitative assessment of P-glycoprotein function in the rat blood-brain barrier by distribution volume of [$^{11}$C]verapamil measured with PET. *Neuroimage* **20**:1775–1782.

Dagenais C, Rousselle C, Pollack GM, and Scherrmann JM (2000) Development of an in situ mouse brain perfusion model and its application to mdr1a P-glycoprotein-deficient mice. *J Cereb Blood Flow Metab* **20**:381–386.

Eichling JO, Raichle ME, Grubb RL Jr, Larson KB, and Ter-Pogossian MM (1975). In vivo determination of cerebral blood volume with radioactive oxygen-15 in the monkey. *Circ Res* **37**:707–714.

Elsinga PH, Hendrikse NH, Bart J, Vaalburg W, and van Waarde A (2004) PET studies on P-glycoprotein function in the blood-brain barrier: how it affects uptake and binding of drugs within the CNS. *Curr Pharm Des* **10**:1493–1503.

Hendrikse N, Schinkel A, de Vries E, Fluks E, Van der Graaf W, Willemsen A, Vaalburg W, and Franssen E (1998) Complete in vivo reversal of P-glycoprotein pump function in the blood- brain barrier visualized with positron emission tomography. *Br J Pharmacol* **124**:1413–1418.

Hendrikse NH, de Vries EG, Eriks-Fluks L, van der Graaf WT, Hospers GA, Willemsen AT, Vaalburg W, and Franssen EJ (1999) A new in vivo method to study P-glycoprotein transport in tumors and the blood-brain barrier. *Cancer Res* **59**: 2411–2416.

Hirrlinger J, Konig J, and Dringen R (2002) Expression of mRNAs of multidrug resistance proteins (Mrps) in cultured rat astrocytes, oligodendrocytes, microglial cells and neurones. *J Neurochem* **82**:716–719.

Kawahara I, Kato Y, Suzuki H, Achira M, Ito K, Crespi CL, and Sugiyama Y (2000) Selective inhibition of human cytochrome P450 3A4 by *N*-[2(*R*)-hydroxy-1(*S*)-indanyl]-5-[2(*S*)-(1,1-dimethylethylaminocarbonyl)-4-[(furo[2, 3-b]pyridin-5-yl)methyl]piperazin-1-yl]-4(*S*)-hydroxy-2(*R*)-phenylmethylpentanamide and P-glycoprotein by valspodar in gene transfectant systems. *Drug Metab Dispos* **28**: 1238–1243.

Kim DC, Sugiyama Y, Satoh H, Fuwa T, Iga T, and Hanano M (1988) Kinetic analysis of in vivo receptor-dependent binding of human epidermal growth factor by rat tissues. *J Pharm Sci* **77**:200–207.

Kortekaas R, Leenders KL, van Oostrom JC, Vaalburg W, Bart J, Willemsen AT, and Hendrikse NH (2005) Blood-brain barrier dysfunction in parkinsonian midbrain in vivo. *Ann Neurol* **57**:176–179.

Kroemer HK, Gautier JC, Beaune P, Henderson C, Wolf CR, and Eichelbaum M (1993) Identification of P450 enzymes involved in metabolism of verapamil in humans. *Naunyn-Schmiedeberg's Arch Pharmacol* **348**:332–337.

Kusuhara H and Sugiyama Y (2001) Efflux transport systems for drugs at the blood-brain barrier and blood-cerebrospinal fluid barrier (part 1). *Drug Discov Today* **6**:150–156.

Kusuhara H, Suzuki H, Terasaki T, Kakee A, Lemaire M, and Sugiyama Y (1997) P-glycoprotein mediates the efflux of quinidine across the blood-brain barrier. *J Pharmacol Exp Ther* **283**:574–580.

Lam FC, Liu R, Lu P, Shapiro AB, Renoir JM, Sharom FJ, and Reiner PB (2001) β-Amyloid efflux mediated by p-glycoprotein. *J Neurochem* **76**:1121–1128.

Link JM (2003) PET imaging of in vivo transporter and receptor activity, in *AAPS Workshop on Drug Transport: From the Bench to the Bedside*, Wyndham Peachtree Conference Center, Peachtree City, GA.

Logan J (2003) A review of graphical methods for tracer studies and strategies to reduce bias. *Nucl Med Biol* **30**:833–844.

Lo Y, Liu F, and Cherng J (2001) Effect of PSC 833 liposomes and Intralipid on the transport of epirubicin in Caco-2 cells and rat intestines. *J Control Release* **76**:1–10.

Maeda J, Suhara T, Ogawa M, Okauchi T, Kawabe K, Zhang MR, Semba J, and Suzuki K (2001) In vivo binding properties of [carbonyl-$^{11}$C]WAY-100635: effect of endogenous serotonin. *Synapse* **40**:122–129.

Obayashi S, Suhara T, Kawabe K, Okauchi T, Maeda J, Akine Y, Onoe H, and Iriki A (2001) Functional brain mapping of monkey tool use. *Neuroimage* **14**:853–861.

Pardridge WM (1988) Recent advances in blood-brain barrier transport. *Annu Rev Pharmacol Toxicol* **28**:25–39.
Pauli-Magnus C, von Richter O, Burk O, Ziegler A, Mettang T, Eichelbaum M, and Fromm MF (2000) Characterization of the major metabolites of verapamil as substrates and inhibitors of P-glycoprotein. *J Pharmacol Exp Ther* **293**:376–382.
Reese TS and Karnovsky MJ (1967) Fine structural localization of a blood-brain barrier to exogenous peroxidase. *J Cell Biol* **34**:207–217.
Rodriguez M, Ortega I, Soengas I, Suarez E, Lukas JC, and Calvo R (2004) Effect of P-glycoprotein inhibition on methadone analgesia and brain distribution in the rat. *J Pharm Pharmacol* **56**:367–374.
Sadeque AJ, Wandel C, He H, Shah S, and Wood AJ (2000) Increased drug delivery to the brain by P-glycoprotein inhibition. *Clin Pharmacol Ther* **68**:231–237.
Sasongko L, Link JM, Muzi M, Mankoff DA, Yang X, Collier AC, Shoner SC, and Unadkat JD (2005) Imaging P-glycoprotein transport activity at the human blood-brain barrier with positron emission tomography. *Clin Pharmacol Ther* **77**:503–514.
Schinkel AH, Smit JJ, van Tellingen O, Beijnen JH, Wagenaar E, van Deemter L, Mol CA, van der Valk MA, Robanus-Maandag EC, te Riele HP, et al. (1994) Disruption of the mouse mdr1a P-glycoprotein gene leads to a deficiency in the blood-brain barrier and to increased sensitivity to drugs. *Cell* **77**:491–502.
Siddiqui A, Kerb R, Weale ME, Brinkmann U, Smith A, Goldstein DB, Wood NW, and Sisodiya SM (2003) Association of multidrug resistance in epilepsy with a polymorphism in the drug-transporter gene ABCB1. *N Engl J Med* **348**:1442–1448.
Song S, Suzuki H, Kawai R, and Sugiyama Y (1999) Effect of PSC 833, a P-glycoprotein modulator, on the disposition of Vincristine and digoxin in rats. *Drug Metab Dispos* **27**:689–694.
Takei M, Kida T, and Suzuki K (2001) Sensitive measurement of positron emitters eluted from HPLC. *Appl Radiat Isot* **55**:229–234.
Tamai I and Tsuji A (2000) Transporter-mediated permeation of drugs across the blood-brain barrier. *J Pharm Sci* **89**:1371–1388.
Tan NC, Heron SE, Scheffer IE, Pelekanos JT, McMahon JM, Vears DF, Mulley JC, and Berkovic SF (2004) Failure to confirm association of a polymorphism in ABCB1 with multidrug-resistant epilepsy. *Neurology* **63**:1090–1092.
Vogelgesang S, Cascorbi I, Schroeder E, Pahnke J, Kroemer HK, Siegmund W, Kunert-Keil C, Walker LC, and Warzok RW (2002) Deposition of Alzheimer's β-amyloid is inversely correlated with P-glycoprotein expression in the brains of elderly non-demented humans. *Pharmacogenetics* **12**:535–541.
von Richter O, Eichelbaum M, Schonberger F, and Hofmann U (2000) Rapid and highly sensitive method for the determination of verapamil, [2H7]verapamil and metabolites in biological fluids by liquid chromatography-mass spectrometry. *J Chromatogr B Biomed Sci Appl* **738**:137–147.
von Richter O, Greiner B, Fromm MF, Fraser R, Omari T, Barclay ML, Dent J, Somogyi AA, and Eichelbaum M (2001) Determination of in vivo absorption, metabolism and transport of drugs by the human intestinal wall and liver with a novel perfusion technique. *Clin Pharmacol Ther* **70**:217–227.
Watanabe M, Okada H, Shimizu K, Omura T, Yoshikawa E, Kosugi T, Mori S, and Yamashita T (1997) A high resolution animal PET scanner using compact PS-PMT detectors. *IEEE Trans Nucl Sci* **44**:1277–1282.
Wegman TD, Maas B, Elsinga PH, and Vaalburg W (2002) An improved method for the preparation of [$^{11}$C]verapamil. *Appl Radiat Isot* **57**:505–507.

**Address correspondence to:** Dr. Tetsuya Suhara, Brain Imaging Project, National Institute of Radiological Sciences, 9-1, Anagawa 4-Chome, Inage-ku, Chiba 263-8555, Japan. E-mail: suhara@nirs.go.jp

# Language Processing and Human Voice Perception in Schizophrenia: A Functional Magnetic Resonance Imaging Study

Michihiko Koeda, Hidehiko Takahashi, Noriaki Yahata, Masato Matsuura, Kunihiko Asai, Yoshiro Okubo, and Hiroshi Tanaka

***Background:*** *Neuroimaging studies have demonstrated either reduced left-lateralized activation or reversed language dominance in schizophrenia. These findings of left hemispheric dysfunction could be attributed to language processing tasks, which activate mainly left hemispheric function. Recent functional magnetic resonance imaging studies reported right-lateralized temporal activation by human voice perception, but few studies have investigated activation by human voice in schizophrenia. We aimed to clarify the cerebral function of language processing in schizophrenia patients by considering cerebral activation of human voice perception.*

***Methods:*** *Fourteen right-handed schizophrenia patients and 14 right-handed controls with matched handedness, sex, and education level were scanned by functional magnetic resonance imaging while listening to sentences (SEN), reverse sentences (rSEN), and identifiable non-vocal sounds (SND).*

***Results:*** *Under the SEN-SND and SEN-rSEN contrasts including language processing, patients showed less activation of the left hemisphere than controls in the language-related fronto-tempo-parietal region, hippocampus, thalamus and cingulate gyrus. Under the rSEN-SND contrast including human voice perception, patients showed less activation than controls in the right-lateralized temporal cortices and bilateral posterior cingulate.*

***Conclusions:*** *Our results indicate that schizophrenia patients have impairment of broader bilateral cortical-subcortical regions related to both the semantic network in the left hemisphere and the voice-specific network in the right hemisphere.*

**Key Words:** Language processing, human voice perception, schizophrenia, semantic network, voice-specific network, functional magnetic resonance imaging (fMRI)

Auditory hallucination and thought disturbance are the main symptoms of schizophrenia and are assumed to be associated with disturbance in language processing (Kircher et al 2002; Mitchell et al 2001; Sommer et al 2001; Woodruff et al 1997). In order to understand the neural basis of these symptoms, achieving the clarification of cerebral function when patients with schizophrenia listen to language will be a challenging target.

Functional magnetic resonance imaging (fMRI) studies have investigated the neural basis of disturbed language processing in schizophrenia (Kasai et al 2003; Kubicki et al 2003; Ragland et al 2004). Functional MRI studies have reported that normal right-handed subjects show left-lateralized activation for language processing (Gaillard et al 2002; Lehericy et al 2000; Schlosser et al 1998), whereas normal left or ambidextrous-handed subjects show bilateral activation for language processing (Hund-Georgiadis et al 2002; Pujol et al 1999; Szaflarski et al 2002). Previous fMRI studies with language listening tasks have demonstrated that schizophrenia patients show either reduced left hemispheric activation (Kiehl and Liddle 2001; Kircher et al 2001) or reversed language dominance (Menon et al 2001; Ngan et al 2003; Woodruff et al 1997), and schizophrenia patients have disturbed left hemisphere dominance for language processing (Sommer et al 2001, 2003). Similarly, fMRI studies with verbal fluency tasks have shown either reduced left frontal activation (Artiges et al 2000; Curtis et al 1998; Yurgelun-Todd et al 1996) or reversed activation in the frontal cortices (Crow 2000; Sommer et al 2001, 2003). These findings of hypo or reversed activation of schizophrenia could depend on the nature of language processing tasks, which mainly activate the left hemisphere in normal subjects.

In schizophrenia, investigating cerebral response to human voice is significant since human voice perception is known to closely associate with the generative mechanism of functional auditory hallucination like languages or specific identifiable sounds (Hayward 2003; Hunter and Woodruff 2004). Recent fMRI studies have shown that the human-voice-specific area is located in the superior temporal sulcus (STS) with right hemisphere dominance in normal subjects (Belin and Zatorre 2003; Belin et al 2002; Belin et al 2000). When auditory hallucination appears, patients with schizophrenia have demonstrated increasing cerebral activation in the temporal cortex (Bentaleb et al 2002; Dierks et al 1999; Woodruff et al 1997). If cerebral activation in the right hemisphere is increased by human voice perception, language dominance in the temporal cortices could be reversed when schizophrenia patients are listening to language. Recent studies have indicated the importance of investigating right-hemisphere language function as a social perception in schizophrenia (Abdi and Sharma 2004; Mitchell and Crow 2005; Onitsuka et al 2005; Williams et al 2004). However, to our knowledge, no studies concerning language processing of schizophrenia have taken cerebral activation by human voice perception into account. Therefore, we investigated how cerebral activation for language processing and human voice perception in schizophrenia patients are different in comparison to normal subjects.

From the Department of Bioinformatics (MK, HTan), Medical Research Institute; Department of Bioinformatics and Computational Biology (HTan), School of Biomedical Sciences; Department of Biofunctional Informatics (MM), Tokyo Medical and Dental University; Department of Pharmacology (NY) and the Department of Neuropsychiatry (YO), Nippon Medical School, Tokyo; National Institute of Radiological Sciences Brain Imaging Project (HTak), Chiba; Asai Hospital (KA), Togane, Japan.

Address reprint requests to Yoshiro Okubo, M.D., Ph.D., Department of Neuropsychiatry, Nippon Medical School, 1-1-5, Sendagi, Bunkyo-ku, Tokyo, 113-8603 Japan; E-mail: okubo-y@nms.ac.jp.

Received August 11, 2005; revised January 6, 2006; accepted January 13, 2006.

0006-3223/06/$32.00
doi:10.1016/j.biopsych.2006.01.013

The aim of our research was to clarify cerebral function by language processing in patients with schizophrenia by considering activation by human voice perception.

## Methods and Materials

### Subjects

Fourteen schizophrenia patients (12 males and 2 females, mean age 31.6 years, SD = 7.0) meeting the DSM-IV criteria for schizophrenia were studied. Diagnoses were made by HTak, YO, and the attending psychiatrists on the basis of a review of their charts and a conventionally semi-structured interview. Exclusion criteria were current or past substance abuse and a history of alcohol-related problems, mood disorder, or organic brain disease. Eleven patients were recruited from the outpatient unit of Asai Hospital, and 3 were recruited from the inpatient unit. Ten of the 14 patients were the same as in our previous fMRI studies investigating emotional neural responses (Takahashi et al 2004). As for the subtypes of schizophrenia, 13 patients were paranoid and one had undifferentiated schizophrenia. Thirteen of the 14 patients were receiving neuroleptics (mean risperidone equivalent daily dosage = 3.6 mg, SD = 3.5; 8 patients, risperidone; 1 patient, perospirone; 1 patient, olanzapine; 1 patient, zotepine; 2 patients, sulpiride), and one was not receiving any neuroleptics. Mean illness duration was 9.6 (SD = 9.7) years. Clinical symptoms were assessed by the Brief Psychiatric Rating Scale (BPRS) (Overall and Gorham 1962). The ratings were reviewed by HTak and YO after the patient interview, and disagreements were resolved by consensus; consensus ratings were used in this study. Further, sum scores for positive and negative symptoms were calculated, with the positive symptom subscale including the following eight items: conceptual disorganization, mannerisms and posturing, hostility, grandiosity, suspiciousness, hallucinatory behavior, unusual thought content, and excitement. The negative symptom subscale included these three items: emotional withdrawal, motor retardation, and blunted affect. The mean score of BPRS was 13.9 (SD = 7.4). The mean positive symptom score was 1.9 (SD = 2.4), and the mean negative symptom score was 3.6 (SD = 2.9). The control group consisted of 14 normal subjects (10 males and 4 females, mean age 29.1 years, SD = 7.8), who were recruited from the surrounding community. The candidates were carefully screened and standardized interviews were conducted by trained psychiatrists (HTak and YO). They did not meet the criteria for any psychiatric disorders. None of the control subjects was taking alcohol or medication at the time, nor did they have a history of psychiatric disorder, significant physical illness, head injury, neurological disorder, or alcohol or drug dependence. Patients tended to have a lower educational status but there was no significant difference in the mean period of education between the controls and patients (mean ± SD; patients 13.2 ± 2.0 years, control subjects 14.4 ± 1.8 years; $p = .15$, $t$-test). All of the patients and control subjects were right-handed, as investigated by the Edinburgh Handedness Inventory (EHI) (mean ± SD; control subjects 92.3 ± 10.3; patients 91.5 ± 9.9, $p > .05$, $t$-test) (Oldfield 1971). Previous fMRI studies defined a right-handed subject as a subject with an EHI score of more than 50 or 52 (Springer et al 1999; Szaflarski et al 2002). Therefore, we defined a right-handed subject as "a subject with an EHI score of more than 52." In our study, 16 patients were initially included, but two ambidextrous patients (EHI: less than 52) were then excluded from the analysis. There was no significant difference in the mean of the EHI score between the two groups. They all underwent MRI to rule out cerebral anatomic abnormalities. After the procedures had been fully explained to the subjects, written informed consent was obtained in accordance with the guidelines of the Asai Hospital Ethics Committee.

### Experimental Design

In a single session, three types of stimuli were presented: forward-played sentences (SEN); reverse sentences (rSEN), the same sentences, but played in reverse; and identifiable nonvocal sounds (SND). The duration of each stimulus was 20 sec, and rSEN, SND, and SEN were played in sequence to each subject. Before each sound, the subjects listened to silence from the headphones for 20 sec (rest condition). Each set was 120 sec, and consisted of these three sound conditions and the rest condition. One session consisted of 8 sets, with a total scanning time of 960 sec (Figure 1). As identifiable non-vocal sounds for the SND condition, sounds of a shower, washing machine, bell, and computer printer were used. The sentences were in Japanese, spoken by two speakers, one male and one female, and represented a single topic per set, with one session consisting of four topics, each repeated twice randomly. Concerning the contents of the sentences, each topic was expressed by one or two sentences, consisting of 6–7 phrases including compound sentences. These sentences used conjunctional phrases or long adjuncts. Therefore, each subject was required to comprehend complex situations and understand the connection of the phrases or sentences (Appendix 1). In our experiment, two voices, one male and one female, were used alternately for the sound contents of sentences and reverse sentences. The material of the sentences included the linguistic section of the contents of Wechsler's Memory Scale – Revised, translated into Japanese (Sugishita 2001; Wechsler 1987). In our research, we used Japanese sentences for Japanese native subjects because research of semantic processing of language has shown left-

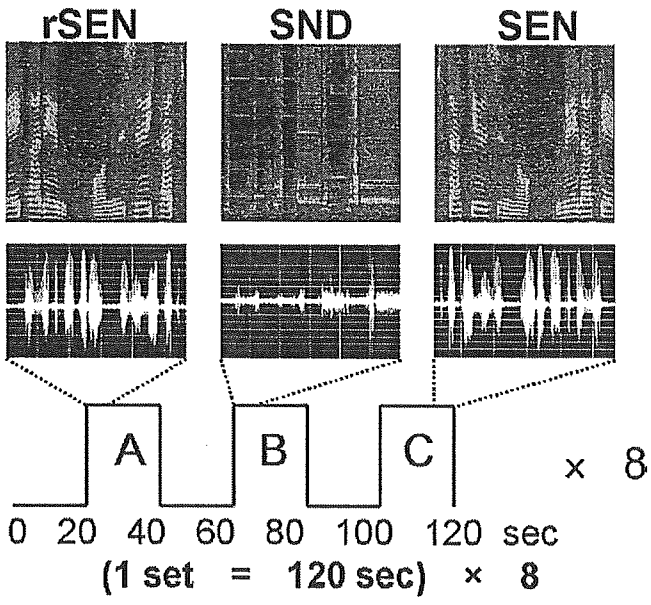


**Figure 1. (A)** Reverse sentences (rSEN), **(B)** Identifiable non-vocal sounds (SND), **(C)** Sentences (SEN). The top row shows sound spectrograms under the three sound conditions. The horizontal axis shows the time domain. The vertical axis shows the frequency (about 15–20000 Hz) of the tone domain. The middle row shows the time-domain waveforms. The horizontal axis shows the tone domain. The vertical axis shows the power of the sound.

lateralized activation in the fronto-tempo-parietal region by native languages (Gaillard et al 2004; Homae et al 2002; Kansaku et al 2000; Springer et al 1999).

We used reverse sentences for the human voice condition. Several phonetics studies have indicated that human voice generated by air passing through the vocal tract or vocal cords has a specific frequency or spectrum of the voice (Joos 1948; Kohler 1984; Simos et al 1997). Reverse sentences have the same spectrum domain as forward sentences (Figure 1) and maintain the character of the human voice. A neuropsychological study has demonstrated that reverse speech is a sound that has very little lexical or semantic information (Binder et al 2000). Additionally, several previous fMRI studies have used reversed speech as non-semantic vocal sound (Burton et al 2001; Howard et al 1992; Price et al 1996). Furthermore, if subjects listen to reverse words or reverse phrases, they may guess the meaning of the term or contents (Burton et al 2001). Therefore, instead of using reverse words or reverse phrases, as non-semantic vocal sound we used reverse sentences of sufficient length to preclude guessing their meaning. We performed a preliminary study in which we asked 30 normal subjects, different from those of this fMRI study, what the reverse sentences sounded like without introducing them in advance (Appendix 2). All subjects answered that the sound was a human voice although they could not understand the contents.

### Instruments Used for Presentation of Stimuli

Stimuli were presented by digital-audio file from a computer. The sounds were presented at 8 bits and the sampling rate was 8 kHz. Subjects listened to the sound stimuli through headphones attached to an air conductance sound delivery system (Commancer X6, MRI Audio System, Resonance Technology Inc., Los Angeles, California).

### Functional MRI Acquisition

The images were acquired with a 1.5 Tesla Signa system (General Electric, Milwaukee, Wisconsin). Functional images of 240 volumes were acquired with T2*-weighted gradient echo planar imaging sequences sensitive to blood oxygenation level dependent (BOLD) contrast. Each volume consisted of 40 transaxial contiguous slices with a slice thickness of 3 mm to cover almost the whole brain (flip angle, 90°; time to echo [TE], 50 msec; repetition time [TR], 4 sec; matrix, 64 × 64; field of view, 24 × 24).

### Behavioral Data

In order to ensure that the subjects actively participated in the fMRI study, each subject was asked a series of questions regarding the contents of each condition (SEN, rSEN, SND) immediately after fMRI scanning. For the SEN condition, the questionnaire consisted of four questions regarding the situation relevant to the sentences, and four questions regarding the proper nouns used in the sentences. For the rSEN condition, the subjects were asked whether they could recognize the sound as human voice, and whether they could discriminate between the voice of a male and a female. For the SND condition, we asked each subject to identify the names of the sound stimuli.

### Image Processing

Data analysis was performed with statistical parametric mapping software SPM2 (Wellcome Department of Cognitive Neurology, London, United Kingdom) running with MATLAB (Mathworks, Natick, Massachusetts). All volumes were realigned to the first volume of each session to correct for subject motion, and they were spatially normalized to the standard space defined by the Montreal Neurological Institute (MNI) template. After normalization, all scans had a final resolution of $3 \times 3 \times 3$ mm$^3$. Functional images were spatially smoothed with a 3-D isotropic Gaussian kernel (full width at half maximum of 8 mm). Low-frequency noise was removed by applying a high-pass filter (cutoff period of 80 sec) to the fMRI time series at each voxel. A temporal smoothing function was applied to the fMRI time series to enhance the temporal signal-to-noise ratio. The significance of hemodynamic changes in each condition was examined using the general linear model with boxcar functions convoluted with a hemodynamic response function. Statistical parametric maps for each contrast of the $t$-statistics were calculated on a voxel-by-voxel basis. The $t$-values were then transformed to unit normal distribution, resulting in $z$-scores.

### Statistical Analysis

Group analysis was performed on the data for 14 control subjects and 14 schizophrenia patients using a random effect model on a voxel-by-voxel basis. Three trials (rSEN, SND, and SEN conditions) were presented by each explanatory variable, and they were each convoluted with a standard hemodynamic response function taken from SPM2 to account for the hemodynamic response lag. At first, we analyzed the one-sample $t$-test for cerebral activation of the control and patient groups, respectively. Second, we investigated the difference of the mean of cerebral activation between control and patient groups using the two-sample $t$-test. The $t$-statistics were calculated for contrast among the three trials.

### Cognitive Systems

To assess the specific condition effect, we used the contrasts of reverse sentences minus identifiable non-vocal sounds (rSEN–SND) and sentences minus identifiable non-vocal sounds (SEN–SND), and sentences minus reverse sentences (SEN-rSEN). In the rSEN-SND and SEN-SND contrasts, we used cerebral activation when the subjects listened to identifiable non-vocal sound (SND) as a baseline in order to investigate whether cerebral activation by language processing or human voice perception was greater than that of listening to non-vocal sound. The contrast of rSEN–SND included human voice perception. The contrast of SEN–SND was assumed to represent the activation due to not only human voice perception but also language processing including lexical-semantic processing. The content of SEN-rSEN was assumed to represent the activation due to lexical-semantic processing (Koeda et al, in press).

A random effect model that estimates the error variance for each condition across the subjects was implemented for group analysis. Contrast images obtained from single-subject analysis were entered into group analysis. A one-sample $t$-test was applied to determine group activation for each effect. Significant clusters of activation were determined using the conjoint expected probability distribution of the height and extent of $z$-scores with the height and extent threshold. Coordinates of activation were converted from MNI coordinates to the Talairach and Tournoux coordinates (Talairach and Tournoux 1988) using the mni2tal algorithm (http://www.mrc-cbu.cam.ac.uk/Imaging/Common/mnispace.shtml).

### Region of Interest (ROI) Analysis

We investigated the activated voxel numbers in the regions of interest (ROIs). The peak coordinates of activation in the control group were used as the common coordinate ROIs for both

controls and patients. Under the SEN-SND and the SEN-rSEN contrasts, ROIs were set at the bilateral triangular portion of IFG (tri-IFG; SEN-SND: [±51, 21, 24], SEN-rSEN: [±48, 18, 24]), the posterior superior temporal gyrus (pSTG; SEN-SND: [±63, −24, 0], SEN-rSEN: [±51, −36, −12]), and the inferior parietal lobe (IPL; SEN-SND: [±42, −72, 36], SEN-rSEN: [±30, −75, 42]). Under the rSEN-SND contrast, ROIs were set at the anterior middle temporal gyrus (aMTG; [±57, 9, −6]). These ROIs were set as spheres of 30-mm radius to clarify the broader cortical activation in the fronto-tempo-parietal region, and statistical threshold was set at random effect model, $p = .001$, uncorrected. Furthermore, we calculated the Laterality Index (LI), which was used in previous fMRI studies (Springer et al 1999; Szaflarski et al 2002) (LI = (L−R) / (L+R) × 100; L: activated voxel numbers in the left hemisphere, R: activated voxel numbers in the right hemisphere) in these regions (threshold: random effect model, $p = .001$, uncorrected). A $p$ value (SEN-SND and SEN-rSEN contrasts: .05/6, rSEN-SND contrast: .05/2) was used in order to prevent type I errors in the multiplicity of statistical analysis.

### Correlation Analysis

We investigated the correlation between cerebral activation of the local area and symptoms of schizophrenia in each patient by using ROI analysis. These ROIs were set as spheres of 20-mm radius to clarify the activation of the specific subcortical regions as well as the cortical regions. We selected the location of each ROI at the peak of cerebral activation of the control group. These ROIs were in the following bilateral sites: frontal lobe (middle frontal gyrus, operculum and triangular gyrus of inferior frontal gyrus), temporal lobe (anterior and posterior areas), parietal lobe, hippocampus, thalamus, and posterior cingulate.

## Results

### Performance

The mean percentages (± SD) of the performance ratio to the questionnaire of the control subjects for SEN, rSEN, and SND were 86.6 ± 12.5%, 89.3 ± 12.8%, and 85.7 ± 12.8%, and those of the schizophrenia patients were 88.3 ± 13.3%, 82.1 ± 11.7%, and 85.7 ± 12.8%, respectively. A mixed analysis of variance (mixed ANOVA) in the percentages of correct answers to the questionnaire did not show a significant difference with one repeated, within-subject factor (type of stimulus): $F$ three contrasts (2,52) = .552, $p = .574 > .05$, one between-subjects factor (group): $F$ groups (1,26) = .349, $p = .560 > .05$, and interaction $F$ contrasts × groups (2,52) = 1.525, $p = .227 > .05$. After the experiment, all control subjects and patients were asked about the difference of gender by listening to reverse sentences made by a male voice and a female voice (Appendix 2). All could discriminate the gender difference.

### Functional MRI Data

**SEN-SND and SEN-rSEN Contrasts.** In the one-sample $t$-test, the control group showed cerebral activation under the SEN-SND contrast in the left middle frontal gyrus (MFG), left IFG, right anterior STS (aSTS), aMTG, left inferior parietal lobe (IPL), left hippocampus, left thalamus, and bilateral posterior cingulate (Figure 2, left column of the SEN-SND contrast, and Table 1 Control subjects: group analysis, random effect model, $p = .001$ uncorrected, extent threshold 50 voxels, $z = 3.31$). On the other hand, cerebral activation of the patient group was observed in the MFG, IFG, and hippocampus in the left hemisphere and bilateral temporal cortices, (Figure 2, middle line of the SEN-SND

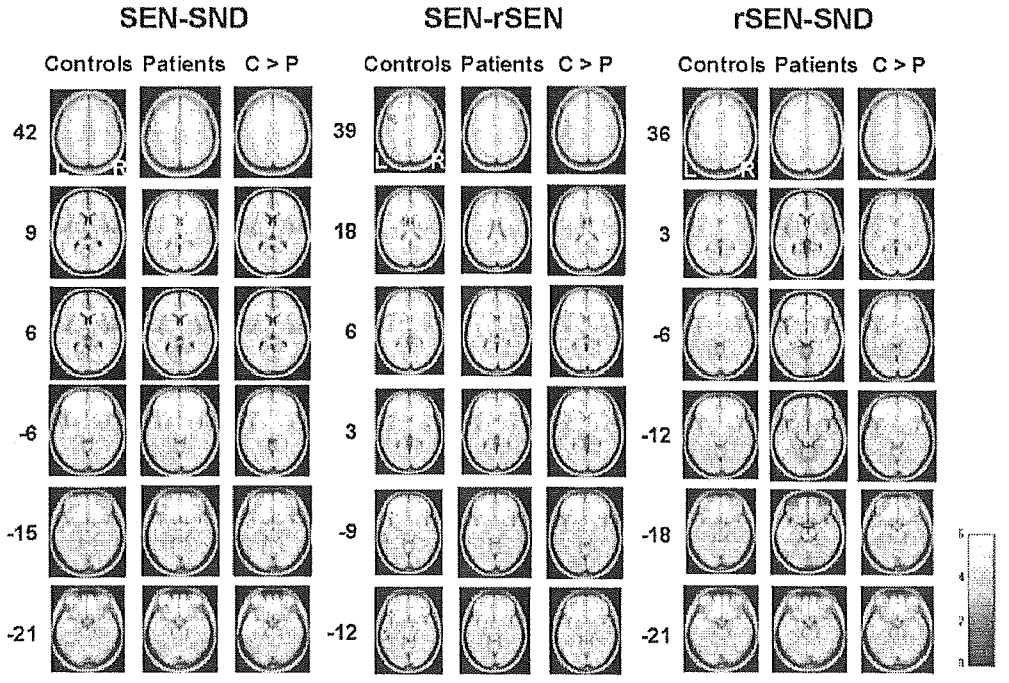


**Figure 2.** Cerebral activation in language processing under SEN-SND and SEN-rSEN contrasts, and cerebral activation in human voice perception under rSEN-SND contrast. In each contrast, the left column shows the results of one-sample $t$-test in control subjects, the middle column shows the results of one-sample $t$-test in schizophrenia patients, and the right column shows the difference of cerebral activation of control subjects over schizophrenia patients by two-sample $t$-test. Numbers along the left side of the columns of the three contrasts represent the $z$ coordinates of Talairach and Tournoux coordinates. rSEN, reverse sentences; SEN, sentences; SND, identifiable non-vocal sounds; C, controls; P, schizophrenia patients.

**Table 1.** Peak Coordinates (X Y Z) and Their *z*-Values of Cerebral Activation Under SEN-SND Contrast in One-Sample *t*-Test of Control Group (Left), in One-Sample *t*-Test of Patient Group (Center), and in Two-Sample *t*-test (Controls > Patients) (Right)

| Contrast | | | SEN-SND | | | | | | | | | | | | | | | | | | | | | |
|---|---|---|---|---|---|---|---|---|---|---|---|---|---|---|---|---|---|---|---|---|---|---|---|---|
| | | | Control Subjects | | | | | | | | Schizophrenia Patients | | | | | | | | Controls > Patients | | | | | | | |
| | | | L | | | | R | | | | L | | | | R | | | | L | | | | R | | | |
| Brain Regions | | | X, | Y, | Z | *z*-value | X, | Y, | Z | *z*-value | X, | Y, | Z | *z*-value | X, | Y, | Z | *z*-value | X, | Y, | Z | *z*-value | X, | Y, | Z | *z*-value |
| Frontal Cortices | | | | | | | | | | | | | | | | | | | | | | | | | | |
| MFG | | BA6/8 | −48, | 6, | 51 | 4.82 | | | | | −42, | 6, | 45 | 3.40 | | | | | −48, | 24, | 42 | 3.08 | | | | |
| IFG | Operculum | BA9/46 | −51, | 21, | 24 | 3.88 | | | | | −45, | 21, | 18 | 3.88 | | | | | −54, | 21, | 24 | 3.36 | | | | |
| IFG | Triangular | BA45/47 | −51, | 24, | −9 | 4.15 | | | | | −48, | 18, | −9 | 3.64 | | | | | −48, | 27, | −6 | 3.68 | | | | |
| Temporal Cortices | | | | | | | | | | | | | | | | | | | | | | | | | | |
| Anterior | STS | BA38 | −52, | 0, | −9 | 4.32 | | | | | | | | | | | | | | | | | | | | |
| | MTG | BA21 | −57, | −3, | −21 | 6.22 | 60, | 6, | −15 | 4.64 | −57, | −12, | −12 | 4.41 | 63, | 0, | −15 | 3.94 | −54, | 3, | −12 | 3.41 | 57, | −3, | −15 | 3.98 |
| | | | | | | | | | | | | | | | | | | | −54, | −33, | −6 | 4.00 | 63, | −9, | −18 | 3.84 |
| Posterior | STS/MTG | BA21/22 | −63, | −24, | 0 | 4.62 | | | | | | | | | | | | | | | | | | | | |
| | MTG | BA21 | −63, | −36, | −3 | 4.94 | 54, | −18, | −15 | 3.34 | −63, | −45, | −9 | 3.31 | 54, | −24, | −12 | 3.34 | −54, | −66, | 9 | 3.47 | 45, | −24, | −4 | 3.26 |
| Parietal Cortices | | | | | | | | | | | | | | | | | | | | | | | | | | |
| Precuneus | | BA19 | −42, | −72, | 36 | 4.82 | | | | | | | | | | | | | −42, | −72, | 36 | 3.57 | | | | |
| Parahippocampus | | BA35 | −18, | −9, | −24 | 4.59 | | | | | −21, | −21, | −21 | 3.82 | | | | | −33, | 0, | −21 | 3.88 | | | | |
| Thalamus | | | −6, | −18, | 9 | 4.59 | | | | | | | | | | | | | −6, | −18, | 9 | 3.88 | | | | |
| Posterior Cingulate | | BA30 | −6, | −57, | 6 | 3.96 | | | | | | | | | | | | | −6, | −60, | 6 | 3.43 | | | | |
| Cerebellum | | | 3, | −75, | −33 | 3.84 | | | | | | | | | | | | | | | | | | | | |

Activation differences were considered significant at height threshold (one-sample *t*-test: $p < .001$, random effect model, uncorrected ($z = 3.31$)) and extent threshold ((50 voxels); two-sample *t*-test: $p < .005$, random effect model, uncorrected, $z = 2.89$). L, left hemisphere; R, right hemisphere; MFG, middle frontal gyrus; IFG, inferior frontal gyrus; STS, superior temporal sulcus; MTG, middle temporal gyrus; BA, Brodmann's area; SEN, sentences; SND, identifiable non-vocal sounds.

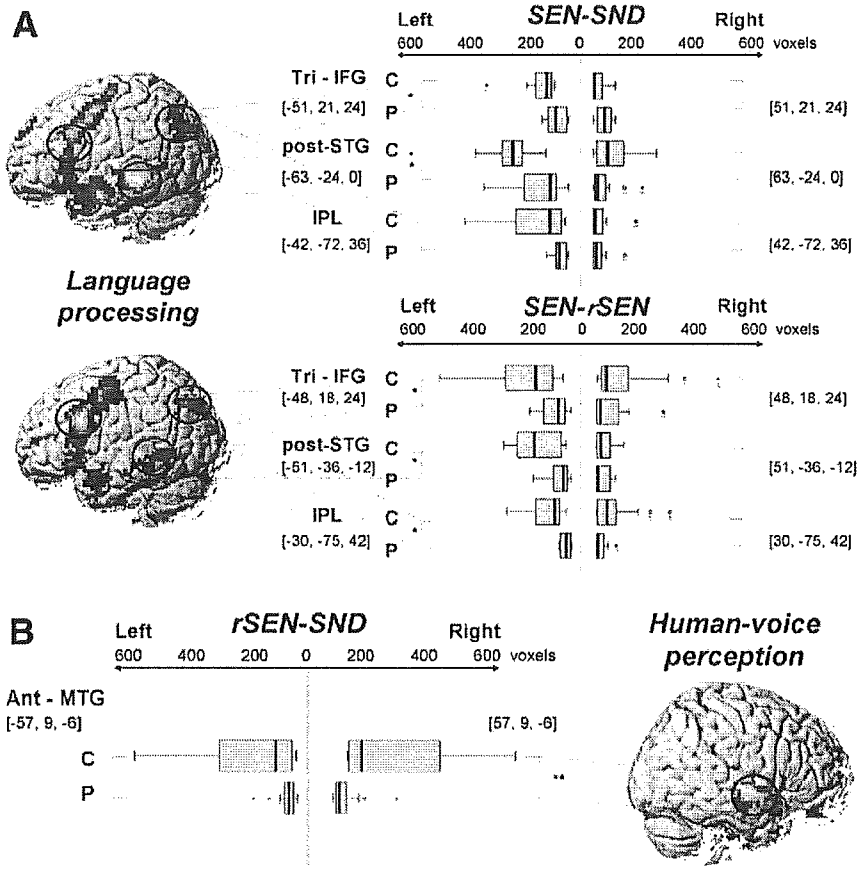


**Figure 3.** Distribution of the activated voxel numbers under the SEN-SND and SEN-rSEN contrasts in the fronto-tempo-parietal lobe **(A)**, and under rSEN-SND contrast in the temporal lobe **(B)** (threshold: $p = .001$, random effect model, uncorrected). From the center line (0 voxel), the left direction shows the left hemispheric-activated voxel numbers, while the right direction shows the right hemispheric-activated voxel numbers. The central coordinates of each ROI are shown on the left and right side of each graph. Each bar shows the 10th and 90th percentiles of distribution from the maximum voxel numbers. Each box shows the 25th, 50th, and 75th percentiles of distribution. The three pictures indicate the results of activation under each contrast in the control group. L, left hemisphere; R, right hemisphere; C, controls; P, schizophrenia patients; tri-IFG, triangular portion of inferior frontal gyrus; aMTG, anterior middle temporal gyrus; pSTG, posterior superior temporal gyrus; IPL, inferior parietal lobe; rSEN, reverse sentences; SEN, sentences; SND, identifiable non-vocal sounds. * $p < .05/6$; ** $p < .05/2$; Bonferroni's multiple comparison.

contrast, and Table 1 Schizophrenia patients: group analysis, random effect model, $p = .001$ uncorrected, extent threshold 50 voxels, $z = 3.31$). In the two-sample $t$-test between the control and patient groups, the patients with schizophrenia showed less activation than the control group in the IFG, posterior MTG, IPL, thalamus, hippocampus, and cingulate in the left hemisphere, but they showed no significantly greater activation in any region (Figure 2, right column of the SEN-SND contrast, and Table 1 Controls > Patients: group analysis, random effect model, $p = .005$ uncorrected, $z = 2.89$).

In the control group, cerebral activation under the SEN-rSEN contrast was observed at the left fronto-tempo-parietal region, and it was similar to that under the SEN-SND contrast. The patient group also showed less activation under the SEN-rSEN contrast, similar to under the SEN-SND contrast. The two-sample $t$ test revealed that the patient group showed less activation than the control group in the left fronto-tempo-parietal region (Figure 2).

Figure 3A (SEN-SND and SEN-rSEN) shows the results of ROI analysis in the tri-IFG, pSTG, and IPL. Table 3 shows the mean ± SD of the activated voxel numbers of the bilateral three regions in the control and patient groups under the SEN-SND and SEN-rSEN contrasts. The volume of the activated area in control subjects was significantly greater than that in schizophrenia patients in the left tri-IFG ($t$-test: $p = .008$ [SEN-SND and SEN-rSEN] $< .05/6$; Bonferroni's multiple comparison), left pSTG ($t$-test: $p = .008$ [SEN-SND], $p = .006$ [SEN-rSEN] $< .05/6$). In the left IPL, patients showed significantly less activation than controls under the SEN-rSEN contrast ($t$-test: $p = .008 < .05/6$), but under the SEN-SND contrast, a significant group difference was not observed ($t$-test: $p = .01 > .05/6$). On the other hand, there was no significant difference between control subjects and schizophrenia patients in the tri-IFG, pSTG, and IPL in the right hemisphere. Figure 4 shows the distribution of laterality index (LI) in the tri-IFG, pSTG, and IPL under the SEN-SND and SEN-rSEN contrasts. The LIs of patients were significantly greater than those of controls in the tri-IFG under the SEN-SND contrast ($t$-test: $p < .001$ ($< .05/6$); Bonferroni's multiple comparison) but not in the other areas ($t$-test: $p > .05/6$).

**Reverse SEN-SND Contrast.** Using the one-sample $t$-test for the rSEN-SND contrast, the control group showed right-lateralized activation in the STS and MTG and bilateral activation in the anterior and posterior cingulate (Figure 2, upper row of the rSEN-SND contrast, and Table 2 Control subjects: group analysis, random effect model, $p = .001$ uncorrected, extent threshold 50 voxels, $z = 3.31$). In contrast, cerebral activation of the patient group was revealed in the bilateral temporal lobe and in the anterior cingulate (Figure 2, middle row of the rSEN-SND contrast, and Table 2 Schizophrenia patients: group analysis, random effect model, $p = .001$ uncorrected, extent threshold 50 voxels, $z = 3.31$). In the two-sample $t$-test between the control and patient groups, the patients demonstrated less right-lateralized activation in the STS and the posterior cingulate than the control group, but they showed no significantly greater activation in any region (Figure 2, lower row of the rSEN-SND contrast, and Table 2 Controls > Patients: group analysis, random effect model, $p = .005$ uncorrected, $z = 2.89$). Figure 3 (rSEN-SND) shows the results of ROI analysis in the aMTG. Table 3 (rSEN-SND) shows the mean ± SD voxel numbers of the control and patient groups in the aMTG. The

**Table 2.** Peaks Coordinates (X Y Z) and Their z-Values of Cerebral Activation Under rSEN-SND Contrast in One-Sample t-Test of Control Group (Left), in One-Sample t-Test of Patient Group (Center), and in Two-Sample t-Test (Controls > Patients) (Right)

| Contrast | | | rSEN-SND | | | | | | | | | | | | | | | | | | | |
|---|---|---|---|---|---|---|---|---|---|---|---|---|---|---|---|---|---|---|---|---|---|---|
| | | | Control Subjects | | | | | | | Schizophrenia Patients | | | | | | | Controls > Patients | | | | | |
| | | | L | | | | R | | | L | | | | R | | | L | | | R | | |
| Brain Regions | | | X, | Y, | Z | z-value | X, | Y, | Z | z-value | X, | Y, | Z | z-value | X, | Y, | Z | z-value | X, | Y, | Z | z-value |
| Temporal Cortices | | | | | | | | | | | | | | | | | | | | | | |
| Anterior | STS | BA38 | | | | | 57, | 9, | −6 | 3.66 | | | | | | | | | 54, | 6, | −21 | 3.63 |
| | MTG | BA21 | | | | | 60, | 3, | −12 | 5.36 | | | | | | | | | | | | |
| Middle | STS | BA22 | −60, | 0, | −3 | 3.63 | | | | | | | | | | | | | 60, | −3, | −18 | 3.16 |
| | MTG | BA21 | −57, | −3, | −9 | 3.36 | 60, | −3, | −6 | 3.41 | −60, | 0, | −12 | 3.32 | 57, | 0, | −9 | 3.46 | | | | |
| Posterior | STS | BA22 | −54, | −24, | 0 | 3.36 | | | | | | | | | | | | | −52, | −30, | −3 | 3.02 |
| | MTG | BA21 | | | | | 57, | −21, | −6 | 3.36 | | | | | | | | | | | | |
| Cingulate | | | | | | | | | | | | | | | 9, | 42, | −9 | 4.82 | | | | |
| Anterior Cingulate | | | −3, | 48, | −9 | 4.75 | | | | | | | | | | | | | −6, | −57, | 24 | 3.34 |
| Posterior Cingulate | | BA 31 | 0, | −57, | 27 | 3.62 | | | | | | | | | | | | | | | | |

Activation differences were considered significant at height threshold (one-sample t-test: $p < .001$, random effect model, uncorrected ($z = 3.31$)) and extent threshold ((50 voxels); two-sample t-test: $p < .005$, random effect model, uncorrected, $z = 2.89$). STS, superior temporal sulcus; MTG, middle temporal gyrus; BA, Brodmann's area; rSEN, reverse sentences; SEN, sentences; SND, identifiable non-vocal sounds.

**Table 3.** Mean ± SD of the Activated Voxel Numbers in Regions of Interest (ROIs)

| Contrast | SEN-SND | | |
|---|---|---|---|
| Region | Left | Right | LI |
| tri-IFG | | | |
| Controls | 99.8 ± 63.3[a] | 19.3 ± 28.0 | 75.2 ± 29.2[a] |
| Patients | 42.8 ± 35.8[a] | 36.2 ± 24.8 | −1.2 ± 61.2[a] |
| pSTG | | | |
| Controls | 219.8 ± 118.8[a] | 67.1 ± 67.0 | 57.7 ± 33.5 |
| Patients | 103.6 ± 89.9[a] | 34.5 ± 46.5 | 37.4 ± 62.9 |
| IPL | | | |
| Controls | 110.8 ± 105.2 | 29.6 ± 49.6 | 64.1 ± 47.7 |
| Patients | 30.6 ± 23.4 | 19.8 ± 28.6 | 26.2 ± 74.3 |
| Contrast | SEN-rSEN | | |
| Region | Left | Right | LI |
| tri-IFG | | | |
| Controls | 218.9 ± 171.5[a] | 116.8 ± 162.9 | 47.0 ± 37.8 |
| Patients | 77.8 ± 61.9[a] | 52.3 ± 81.5 | 36.9 ± 63.9 |
| pSTG | | | |
| Controls | 152.6 ± 102.7[a] | 33.1 ± 36.7 | 69.3 ± 28.8 |
| Patients | 58.9 ± 54.8[a] | 27.2 ± 31.9 | 39.6 ± 58.9 |
| IPL | | | |
| Controls | 109.4 ± 79.8[a] | 75.7 ± 96.8 | 39.2 ± 52.7 |
| Patients | 28.5 ± 25.1[a] | 18.6 ± 24.6 | 32.9 ± 69.5 |
| Contrast | rSEN-SND | | |
| Region | Left | Right | LI |
| aMTG | | | |
| Controls | 158.4 ± 179.7 | 210.7 ± 196.2[b] | −25.6 ± 39.0 |
| Patients | 43.7 ± 44.7 | 46.6 ± 62.1[b] | 7.5 ± 56.0 |

L, left hemisphere; R, right hemisphere; LI, Laterality Index; tri-IFG, triangular portion of inferior frontal gyrus; pSTG, posterior superior temporal gyrus; IPL, inferior parietal lobe; aMTG, anterior middle temporal gyrus.
[a] $p < .05/6$, Bonferroni's multiple comparison.
[b] $p < .05/2$, Bonferroni's multiple comparison.

ROI volume in controls was significantly greater than that in patients in the right aMTG (right aMTG: t-test: $p = .004 < .05/2$; Bonferroni's multiple comparison), but not in the left aMTG (left aMTG: t-test: $p > .05/2$). The LI distribution was not significantly different between controls and patients in the aMTG (t-test: $p > .05/2$, Figure 4).

### Correlation Analysis

We investigated the correlation between cerebral activation of local areas and symptoms of schizophrenia (total score of BPRS, positive symptoms and negative symptoms). However, no significant correlation was observed in any area (Spearman's correlation coefficient: $p > .05$). In addition, significant correlations were not seen between LI and the BPRS score in any area (Spearman's correlation coefficient: $p > .05$).

## Discussion

To clarify the cerebral function of language processing in patients with schizophrenia by considering cerebral activation of human voice perception, we investigated the difference of cerebral activation between right-handed control subjects and right-handed schizophrenia patients while they were listening to SEN, rSEN, and SND. Under the SEN-SND and SEN-rSEN contrasts, including language processing, the patients demonstrated less cerebral activation

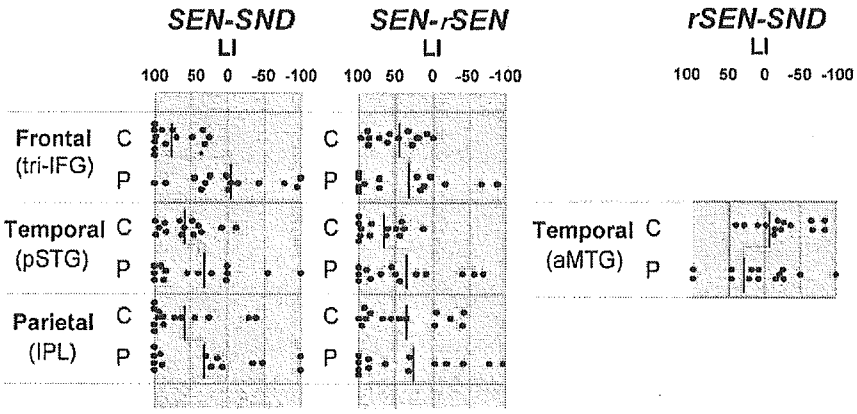


**Figure 4.** Distribution of the Laterality Index (LI) in individual subjects under the three contrasts. Each bar shows the mean of individual LIs. C, controls; P, schizophrenia patients; tri-IFG, triangular portion of inferior frontal gyrus; aMTG, anterior middle temporal gyrus; pSTG, posterior superior temporal gyrus; IPL inferior parietal lobe; rSEN, reverse sentences; SEN, sentences; SND, identifiable non-vocal sounds. * $p < .05/6$; Bonferroni's multiple comparison.

than the controls in the fronto-tempo-parietal region, hippocampus, thalamus and cingulate in the left hemisphere. Further, under the rSEN-SND contrast, which includes human voice perception, the patients demonstrated less activation than controls in the right STS, right MTG, and bilateral posterior cingulate.

### Language Processing in Schizophrenia

The results of fMRI studies of schizophrenia have demonstrated two patterns of cerebral activation for language processing. One is reduced left hemispheric activation (Gaillard et al 2002; Kiehl and Liddle 2001; Kircher et al 2001; Lehericy et al 2000; Schlosser et al 1998), and the other is the reversal of normal language dominance (Crow 2000; Dollfus et al 2005; Menon et al 2001; Ngan et al 2003; Sommer et al 2001, 2003; Woodruff et al 1997). In accordance with the former, our patient group showed less activation of the left hemisphere for language processing than the control group in the fronto-tempo-parietal region, thalamus, and cingulate. Numerous fMRI studies of normal subjects have demonstrated that the left tri-IFG, left pSTG, and left IPL were activated by lexical-semantic processing while listening to speech (Binder et al 1997; Price 2000; Schlosser et al 1999). Reduced activation of the left hemisphere in schizophrenia patients compared with control subjects could be considered to represent dysfunction of the semantic network in the fronto-tempo-parietal cortex associated with language processing.

Although our ROI analysis demonstrated significantly lower LI in the tri-IFG under the SEN-SND contrast in patients than in controls, we did not observe hyper-activation in the right hemisphere. Thus, the lower frontal LI in schizophrenia patients could be attributed to left hemispheric hypo-activation during language processing (Figure 3, Figure 4, Table 3).

### Human Voice Perception of Schizophrenia

We confirmed that reverse sentences were perceived as 'human voice' and 'non-semantic information' in a separate preliminary study. All subjects of the preliminary study recognized the sound as a human voice although they could not understand the contents. Therefore, we adopted the rSEN-SND contrast as a condition of human voice perception without semantic processing.

Patients with schizophrenia have a dysfunction in the ability to discriminate between their own voice and another person's voice (Allen et al 2004). Functional MRI studies of normal subjects demonstrated that the human voice-specific area was located in the STS, dominantly in the right hemisphere (Belin and Zatorre 2003; Belin et al 2000, 2002; von Kriegstein et al 2003; Zatorre et al 2004). However, there are few studies to investigate cerebral response specifically to human voice. One psychological study has indicated that voice recognition, including emotion, is impaired in subjects with schizophrenia (Morrison and Wells 2003). Another fMRI study suggested that the normal right-lateralized response due to emotional prosody is reversed when schizophrenia patients recognize emotional prosody of sentences (Mitchell et al 2004). Since schizophrenia patients showed increased cerebral activation in the temporal cortex during auditory hallucination (Bentaleb et al 2002; Dierks et al 1999; Woodruff et al 1997), we supposed that cerebral activation in such patients would be greater than that in control subjects. However, contrary to our expectations, cerebral activation under the rSEN-SND contrast in patients showed less activation than controls in the right STS, right MTG, and posterior cingulate, although the mean of the performance ratio to human voice was not significantly different. Our present finding of less activation indicates that cerebral activation to human voice was disturbed in schizophrenia patients, suggesting that patients have impairment of broader bilateral cortical and subcortical regions, accompanied by dysfunction of both the semantic network in the left hemisphere and the voice-specific network in the right hemisphere.

Our present study has limitations. First, most of the patients were taking neuroleptic medications, possibly affecting neural activation. They were, however, taking atypical neuroleptics at relatively low doses. To our knowledge, there have been no previous studies on the effect of neuroleptics on the BOLD response of language processing and human voice perception. Atypical neuroleptics have shown less influence on BOLD contrast in the motor cortex or the thalamus during a finger-tapping procedure as compared to typical neuroleptics (Braus et al 1999; Muller and Klein 2000). Second, we could not demonstrate any correlation between signal changes and BPRS scores in patients, possibly due to a lack of dispersion in the psychopathology of the patients, most of them being outpatients with mild psychiatric symptoms. Third, recent fMRI studies discussed gender differences of cerebral activation in language processing (Gur et al 2000; Kansaku et al 2000; Shaywitz et al 1995; Sommer et al 2003). These studies demonstrated reduced language dominance in normal female groups in comparison with normal male groups. We could not evaluate the influence of gender differences in our study, because only two of the fourteen patients were female. Since there have been few studies concerning the influence of gender differences on language dominance in schizophrenia, this point would need to be investigated in the future.

When cerebral function in language processing was investigated, cerebral activation of right-handed patients with schizo-

phrenia was less than controls in the broader language-associated areas, including the left IFG, left posterior MTG, left IPL, left thalamus, left hippocampus, and bilateral posterior cingulate. The patient group did not show greater activation than the control group in any language-associated area. Furthermore, in cerebral activation of human voice perception, the patient group demonstrated less activation than the control group in the right STS, right MTG, and bilateral cingulate. These findings indicate that right-handed schizophrenia patients have a disturbance of both left hemispheric function for language processing and right hemispheric function for human voice perception.

*We gratefully acknowledge the staffs of the Section of Biofunctional Informatics, Graduate School of Medicine, Tokyo Medical and Dental University, and of Asai Hospital.*

*This work was supported by a Grant-in-Aid for Scientific Research from the Japanese Ministry of Education, Culture, Sports, Science and Technology (11B-3), a Research Grant for Nervous and Mental Disorders (14B-3), and a Health and Labor Sciences Research Grant for Research on Psychiatric and Neurological Diseases and Mental Health (H15-kokoro-03) from the Japanese Ministry of Health, Labor and Welfare.*

Abdi Z, Sharma T (2004): Social cognition and its neural correlates in schizophrenia and autism. *CNS Spectr* 9:335–343.

Allen PP, Johns LC, Fu CH, Broome MR, Vythelingum GN, McGuire PK (2004): Misattribution of external speech in patients with hallucinations and delusions. *Schizophr Res* 69:277–287.

Artiges E, Martinot JL, Verdys M, Attar-Levy D, Mazoyer B, Tzourio N, et al (2000): Altered hemispheric functional dominance during word generation in negative schizophrenia. *Schizophr Bull* 26:709–721.

Belin P, Zatorre RJ (2003): Adaptation to speaker's voice in right anterior temporal lobe. *Neuroreport* 14:2105–2109.

Belin P, Zatorre RJ, Ahad P (2002): Human temporal-lobe response to vocal sounds. *Brain Res Cogn Brain Res* 13:17–26.

Belin P, Zatorre RJ, Lafaille P, Ahad P, Pike B (2000): Voice-selective areas in human auditory cortex. *Nature* 403:309–312.

Bentaleb LA, Beauregard M, Liddle P, Stip E (2002): Cerebral activity associated with auditory verbal hallucinations: a functional magnetic resonance imaging case study. *J Psychiatry Neurosci* 27:110–115.

Binder JR, Frost JA, Hammeke TA, Bellgowan PS, Springer JA, Kaufman JN, et al (2000): Human temporal lobe activation by speech and nonspeech sounds. *Cereb Cortex* 10:512–528.

Binder JR, Frost JA, Hammeke TA, Cox RW, Rao SM, Prieto T (1997): Human brain language areas identified by functional magnetic resonance imaging. *J Neurosci* 17:353–362.

Braus DF, Ende G, Weber-Fahr W, Sartorius A, Krier A, Hubrich-Ungureanu P, et al (1999): Antipsychotic drug effects on motor activation measured by functional magnetic resonance imaging in schizophrenic patients. *Schizophr Res* 39:19–29.

Burton MW, Noll DC, Small SL (2001): The anatomy of auditory word processing: individual variability. *Brain Lang* 77:119–131.

Crow TJ (2000): Invited commentary on: functional anatomy of verbal fluency in people with schizophrenia and those at genetic risk. The genetics of asymmetry and psychosis. *Br J Psychiatry* 176:61–63.

Curtis VA, Bullmore ET, Brammer MJ, et al (1998): Attenuated frontal activation during a verbal fluency task in patients with schizophrenia. *Am J Psychiatry* 155:1056–1063.

Dierks T, Linden DE, Jandl M, Formisano E, Goebel R, Lanfermann H, et al (1999): Activation of Heschl's gyrus during auditory hallucinations. *Neuron* 22:615–621.

Dollfus S, Razafimandimby A, Delamillieure P, Brazo P, Joliot M, Mazoyer B, et al (2005): Atypical hemispheric specialization for language in right-handed schizophrenia patients. *Biol Psychiatry* 57:1020–1028.

Gaillard WD, Balsamo L, Xu B, Grandin CB, Braniecki SH, Papero PH, et al (2002): Language dominance in partial epilepsy patients identified with an fMRI reading task. *Neurology* 59:256–265.

Gaillard WD, Balsamo L, Xu B, McKinney C, Papero PH, Weinstein S, et al (2004): fMRI language task panel improves determination of language dominance. *Neurology* 63:1403–1408.

Gur RC, Alsop D, Glahn D, Petty R, Swanson CL, Maldjian JA, et al (2000): An fMRI study of sex differences in regional activation to a verbal and a spatial task. *Brain Lang* 74:157–170.

Hayward M (2003): Interpersonal relating and voice hearing: to what extent does relating to the voice reflect social relating? *Psychol Psychother* 76: 369–383.

Homae F, Hashimoto R, Nakajima K, Miyashita Y, Sakai KL (2002): From perception to sentence comprehension: the convergence of auditory and visual information of language in the left inferior frontal cortex. *Neuroimage* 16:883–900.

Howard D, Patterson K, Wise R, Brown WD, Friston K, Weiller C, Frackowiak R (1992): The cortical localization of the lexicons. Positron emission tomography evidence. *Brain* 115:1769–1782.

Hund-Georgiadis M, Lex U, Friederici AD, von Cramon DY (2002): Noninvasive regime for language lateralization in right- and left-handers by means of functional MRI and dichotic listening. *Exp Brain Res* 145:166–176.

Hunter MD, Woodruff PW (2004): Characteristics of functional auditory hallucinations. *Am J Psychiatry* 161:923.

Joos M (1948): Acoustic phonetics. *Lang Monogr* 23:1–137.

Kansaku K, Yamaura A, Kitazawa S (2000): Sex differences in lateralization revealed in the posterior language areas. *Cereb Cortex* 10:866–872.

Kasai K, Yamada H, Kamio S, Nakagome K, Iwanami A, Fukuda M, et al (2003): Neuromagnetic correlates of impaired automatic categorical perception of speech sounds in schizophrenia. *Schizophr Res* 59:159–172.

Kiehl KA, Liddle PF (2001): An event-related functional magnetic resonance imaging study of an auditory oddball task in schizophrenia. *Schizophr Res* 48:159–171.

Kircher TT, Liddle PF, Brammer MJ, Williams SC, Murray RM, McGuire PK (2001): Neural correlates of formal thought disorder in schizophrenia: preliminary findings from a functional magnetic resonance imaging study. *Arch Gen Psychiatry* 58:769–774.

Kircher TT, Liddle PF, Brammer MJ, Williams SC, Murray RM, McGuire PK (2002): Reversed lateralization of temporal activation during speech production in thought disordered patients with schizophrenia. *Psychol Med* 32:439–449.

Koeda M, Takahashi H, Yahata N, Asai K, Okubo Y, Tanaka H, et al (in press): An fMRI Study: Cerebral Laterality for Lexical-Semantic Processing and Human Voice Perception. *AJNR Am J Neuroradiol.*

Kohler KJ (1984): Phonetic explanation in phonology: the feature fortis/lenis. *Phonetica* 41:150–174.

Kubicki M, McCarley RW, Nestor PG, Huh T, Kikinis R, Shenton ME, Wible CG (2003): An fMRI study of semantic processing in men with schizophrenia. *Neuroimage* 20:1923–1933.

Lehericy S, Cohen L, Bazin B, Samson S, Giacomini E, Rougetet, et al (2000): Functional MR evaluation of temporal and frontal language dominance compared with the Wada test. *Neurology* 54:1625–1633.

Menon V, Anagnoson RT, Mathalon DH, Glover GH, Pfefferbaum A (2001): Functional neuroanatomy of auditory working memory in schizophrenia: relation to positive and negative symptoms. *Neuroimage* 13:433–446.

Mitchell RL, Crow TJ (2005): Right hemisphere language functions and schizophrenia: the forgotten hemisphere? *Brain* 128:963–978.

Mitchell RL, Elliott R, Barry M, Cruttenden A, Woodruff PW (2004): Neural response to emotional prosody in schizophrenia and in bipolar affective disorder. *Br J Psychiatry* 184:223–230.

Mitchell RL, Elliott R, Woodruff PW (2001): fMRI and cognitive dysfunction in schizophrenia. *Trends Cogn Sci* 5:71–81.

Morrison AP, Wells A (2003): A comparison of metacognitions in patients with hallucinations, delusions, panic disorder, and nonpatient controls. *Behav Res Ther* 41:251–256.

Muller JL, Klein HE (2000): Neuroleptic therapy influences basal ganglia activation: a functional magnetic resonance imaging study comparing controls to haloperidol- and olanzapine-treated inpatients. *Psychiatry Clin Neurosci* 54:653–658.

Ngan ET, Vouloumanos A, Cairo TA, Laurens KR, Bates AT, Anderson CM, et al (2003): Abnormal processing of speech during oddball target detection in schizophrenia. *Neuroimage* 20:889–897.

Oldfield RC (1971): The assessment and analysis of handedness: the Edinburgh inventory. *Neuropsychologia* 9:97–113.

Onitsuka T, Nestor PG, Gurrera RJ, Shenton ME, Kasai K, Frumin M, et al (2005): Association between reduced extraversion and right posterior

fusiform gyrus gray matter reduction in chronic schizophrenia. *Am J Psychiatry* 162:599–601.
Overall JE, Gorham OR (1962): The brief psychiatric rating scale. *Psych Res* 10:799–812.
Price CJ (2000): The anatomy of language: contributions from functional neuroimaging. *J Anat* 197:335–359.
Price CJ, Wise RJ, Warburton EA, Moore CJ, Howard D, Patterson K, et al (1996): Hearing and saying. The functional neuro-anatomy of auditory word processing. *Brain* 119:919–31.
Pujol J, Deus J, Losilla JM, Capdevila A (1999): Cerebral lateralization of language in normal left-handed people studied by functional MRI. *Neurology* 52:1038–1043.
Ragland JD, Gur RC, Valdez J, Turetsky BI, Elliott M, Kohler C, et al (2004): Event-related fMRI of frontotemporal activity during word encoding and recognition in schizophrenia. *Am J Psychiatry* 161:1004–1015.
Schlosser MJ, Luby M, Spencer DD, Awad IA, McCarthy G (1999): Comparative localization of auditory comprehension by using functional magnetic resonance imaging and cortical stimulation. *J Neurosurg* 91:626–635.
Schlosser R, Hutchinson M, Joseffer S, Rusinek H, Saarimaki A, Stevenson J, et al (1998): Functional magnetic resonance imaging of human brain activity in a verbal fluency task. *J Neurol Neurosurg Psychiatry* 64:492–498.
Shaywitz BA, Shaywitz SE, Pugh KR, Constable RT, Skudlarski P, Fulbright RK, et al (1995): Sex differences in the functional organization of the brain for language. *Nature* 373:607–609.
Simos PG, Molfese DL, Brenden RA (1997): Behavioral and electrophysiological indices of voicing-cue discrimination: laterality patterns and development. *Brain Lang* 57:122–150.
Sommer IE, Ramsey NF, Kahn RS (2001): Language lateralization in schizophrenia, an fMRI study. *Schizophr Res* 52:57–67.
Sommer IE, Ramsey NF, Mandl RC, Kahn RS (2003): Language lateralization in female patients with schizophrenia: an fMRI study. *Schizophr Res* 60:183–190.
Springer JA, Binder JR, Hammeke TA, Swanson SJ, Frost JA, Bellgowan PS, et al (1999): Language dominance in neurologically normal and epilepsy subjects: a functional MRI study. *Brain* 122:2033–2046.
Sugishita M (2001): The Japanese Version of the Wechsler Memory Scale-Revised. Tokyo, Japan: Nihon Bunka Kaga Kusya.
Szaflarski JP, Binder JR, Possing ET, McKiernan KA, Ward BD, Hammeke TA (2002): Language lateralization in left-handed and ambidextrous people: fMRI data. *Neurology* 59:238–244.
Takahashi H, Koeda M, Oda K, Matsuda T, Matsushima E, Matsuura M, et al (2004): An fMRI study of differential neural response to affective pictures in schizophrenia. *Neuroimage* 22:1247–1254.
Talairach J, Tournoux P (1988): Co-Planar Stereotaxic Atlas of the Human Brain: Three Dimensional Proportional System. New York: Thieme Medical.
von Kriegstein K, Eger E, Kleinschmidt A, Giraud AL (2003): Modulation of neural responses to speech by directing attention to voices or verbal content. *Brain Res Cogn Brain Res* 17:48–55.
Wechsler D (1987): Wechsler Memory Scale-Revised. San Antonio, Texas: Harcourt Brace Jovanovich.
Williams LM, Das P, Harris AW, Liddell BB, Brammer MJ, Olivieri G, et al (2004): Dysregulation of arousal and amygdala-prefrontal systems in paranoid schizophrenia. *Am J Psychiatry* 161:480–489.
Woodruff PW, Wright IC, Bullmore ET, Brammer M, Howard RJ, Williams SC, et al (1997): Auditory hallucinations and the temporal cortical response to speech in schizophrenia: a functional magnetic resonance imaging study. *Am J Psychiatry* 154:1676–1682.
Yurgelun-Todd DA, Waternaux CM, Cohen BM, Gruber SA, English CD, Renshaw PF (1996): Functional magnetic resonance imaging of schizophrenic patients and comparison subjects during word production. *Am J Psychiatry* 153:200–205.
Zatorre RJ, Bouffard M, Belin P (2004): Sensitivity to auditory object features in human temporal neocortex. *J Neurosci* 24:3637–3642.

## Appendix 1.

We used the following sentences in the task.

1. Ms. Keiko Ueda, who lives in Kitakyushu City and works as a licensed cook at a company cafeteria, notified the police near the station that 56,000 yen were stolen when she was mugged at Odouri last night.
2. Last night, when Mr. Ichiro Sato was driving a 10-ton truck full of eggs along the road to Yokohama, near the mouth of the Tama River the axle of the truck broke, and the truck slipped off the road and was buried in a ditch.
3. These days "Casual Day" during which businessmen work in plain clothes with no tie has been established, but the apparel business has developed and is marketing a "Dressed Up Monday Campaign" that advertises "Let's be smartly dressed in a suit every Monday."
4. Today, the designs of Northern Europe have become increasingly popular, and a cultural event showing a collection of Swedish designs, music and images, etc., called 'Swedish style 2001,' will be held at various locations in Tokyo.

## Appendix 2.

### Questionnaire

Please answer the following question after listening to two sounds.

1. **As what did you recognize these sounds? Please circle the appropriate one.**

(1) Human voice
(2) Animal sound
(3) Machine sound
(4) Environmental sound

2. **If you circled No. (1), please answer these questions.**

As what did you recognize the first sound?

(1) Male voice
(2) Female voice

As what did you recognize the second sound?

(1) Male voice
(2) Female voice

3. **Did you recognize these sounds as having intonation?**

Yes No

4. **Did you recognize a message from these sounds?**

Yes No